

Immobilization of Reporter Bacteriophage PPO1 on Electrospun Polyhydroxybutyrate Fiber for
Escherichia coli O157:H7 detection

by

Sim Yee Chen

A thesis submitted in partial fulfillment of the requirements for the degree of

Master of Science

in

Chemical Engineering

Department of Chemical and Materials Engineering
University of Alberta

© Sim Yee Chen, 2019

Abstract

Food pathogens are the main sources of food poisoning. Among the pathogens, *Escherichia coli* (*E. coli*) O157:H7 is a Shiga toxin-producing bacterium that leads to thousand of illnesses. Most infection cases are related to consuming undercooked contaminated food products. People of any age can be infected. Symptoms of infections includes severe stomach cramps, diarrheas and may lead to kidney failure.

The current detection methods of *E.coli* O157:H7 provides a sensitive tool to detect low number of cells, however, they are time consuming (48 to 72 h), labor intensive and require professionals in handling and interpreting the results. Therefore, a portable biosensor that can report results rapidly are desired. Here we propose a bacteriophage (phage)-based detection method using engineered NanoLuc reporter phages, namely PPO1, immobilized on electrospun poly-3-hydroxybutyrate (PHB). The engineered reporter phages express a luminescent protein when *E. coli* O157:H7 cells are infected, indicating the presence of target pathogens during enrichment period. To implement phages in this application, it is desirable to immobilize them on a substrate to serve as a swab. For the swab application, high density of immobilized phages are required to generate detectable signal. Previous work has looked at phage immobilization on PHB substrate and found that plasma treated polymer thin film enables immobilization of phages on the polymer substrate. In this work, it is hypothesized that higher phage loading on the polymer substrate could be achieved from porous electrospun mats, increasing the sensitivity of the biosensor.

Infectivity of immobilized phages on 4 different substrates: 2 solvent casted and 2 electrospun from 1 and 5 % w/v PHB in chloroform, were studied. Porous nonwoven microfibers PHB mats were produced from electrospinning. Flat PHB films were solvent-casted and plasma treated. Phages were immobilized on PHB substrates by immersing substrates in 10^8 PFU/ml of phage suspension at 4 °C overnight. To study the infectivity of immobilized phages, *E. coli* infection

dynamic assays were carried out. A bioluminescence assay was conducted with the most promising material samples to validate the bacterial sensing property of the phage-immobilized PHB substrates in detecting *E. coli* O157:H7. We found that immobilized phages on electrospun fibers from 5 % w/v PHB solution displayed higher infectivity than that of phages on plasma-treated flat film in the *E. coli* infection dynamic assays. In the bioluminescence assay, immobilized phages on electrospun fibers detected *E. coli* cells at a concentration of 10^3 CFU/ml within 3 hours in milk, a complex medium.

We anticipate our phage-immobilized PHB to be a starting point for more sophisticated biosensors. For example, phage cocktails, which is to combine two or more phages, could be immobilized on the substrates for diverse host range. Furthermore, the phage-immobilized PHB substrate also has a potential use as antimicrobial packaging. In conclusion, microstructures of the electrospun PHB increased infectivity of immobilized phages on the substrate and may play a key role in supporting other phage-immobilized applications.

Acknowledgements

I would like to begin by expressing my deep gratitude to my advisors, Dr. Anastasia Elias and Dr. Dominic Sauvageau, for being my mentors as I pursued my MSc., for the encouragement, guidance and continuous support of my project. Thank you for guiding me and challenging milestones in my project. I would also like to thank my defense chair, Dave Sharp, and defense committee, Dr. Anastasia Elias, Dr. Dominic Sauvageau and Dr. Ravin Narain for their valuable time and support.

To various people who had supported me during my work, thank you for your expertise, insights and guidance. Among them, Dr. John Nychka, Dr. Jingli Luo, Dr. Hyun-Joong Chung and lab members from these labs for training and providing equipment used in this study. In particular, I want to sincerely thank Eng Khoon Ng for his continued advice and technical skills throughout my project. I am also extremely grateful to my friends and colleagues from the Elias and Dominic research groups who contributed to the discussion of this thesis content.

Lastly, and most of all, my parents deserve special mention for their continual support and love throughout my life.

Table of Contents

Abstract.....	ii
Acknowledgments.....	iv
List of Tables	ix
List of Figures.....	x
Nomenclature and Abbreviations	xiii
Symbols.....	xiii
Abbreviations.....	xiii
1. Introduction.....	1
1.1 Background and Motivation	1
1.2 Objectives of Study.....	4
1.3 Organization of the Report.....	5
2. Literature Review.....	6
2.1 <i>E. coli</i> Detection.....	6
2.2 Bacteriophage-based Biosensors.....	9
2.3 Luciferase Reporter Phages.....	12
2.4 Phage Immobilization.....	14
2.4.1 Challenges in Phage Immobilization.....	15
2.4.2 Application of Phage Immobilization.....	17
2.5 Poly-3-hydroxybutyrate.....	19

2.5.1 Introduction to Poly-3-hydroxybutyrate.....	19
2.6 Electrospinning of PHB.....	21
2.6.1 Introduction to Electrospinning.....	22
2.6.2 Literature Review of Electrospun PHB.....	26
3. Materials and Methods.....	28
3.1 Materials.....	29
3.2 Preparation of Samples.....	30
3.2.1 Preparation of PHB Solution in Chloroform.....	30
3.2.2 Electrospun PHB Substrates.....	31
3.2.3 Solvent-cast Plasma Treated PHB Substrates.....	34
3.2.4 <i>E. coli</i> O157:H7 Overnight Culture.....	35
3.2.5 Fresh Log-phase <i>E. coli</i> O157:H7 Culture.....	35
3.2.6 Phage Amplification.....	36
3.2.7 Phage Immobilization on PHB Substrates.....	37
3.2.8 Washing of Phage-immobilized Substrates.....	37
3.3 Characterization.....	37
3.3.1 Scanning Electron Microscope.....	37
3.3.2 Water Contact Angle Measurement.....	38
3.3.3 Double Agar Plaque Assay.....	38
3.3.4 Phage Loading.....	39

3.3.5 Release Phages.....	39
3.3.6 Fluorescent Confocal Laser Scanning Microscopy.....	39
3.3.7 Helium Ion Microscopy.....	40
3.3.8 <i>E. coli</i> Infection Dynamics.....	41
3.3.9 Bioluminescence Assay.....	41
3.3.10 <i>E. coli</i> Capture Test.....	42
3.3.11 Bioluminescence Assay of Electrospun Fiber Mats.....	42
3.3.12 Swab Test of Electrospun Fiber Mats.....	42
4. Results and Discussion.....	44
4.1 PHB Sample Characterization.....	44
4.2 Wettability.....	47
4.3 Phage Loading.....	49
4.4 Phage Release after Immobilization.....	50
4.5 Phage Attachment on PHB Substrates.....	51
4.6 Phage Distribution on PHB Substrates.....	53
4.7 Phage Activity on PHB Substrates.....	54
4.8 <i>E. coli</i> Detection in Cultures.....	56
4.9 Performance of Phage-based Material for <i>E. coli</i> O157:H7 Detection.....	57
4.10 Discussion on Phage Attachment.....	61
4.11 Comparison of Efficiency of Phage-loading Substrates.....	63

4.12 Immobilized Reporter Phages for the Detection of <i>E.coli</i> O157:H7	65
5. Conclusions.....	68
5.1 Summary.....	68
5.2 Significance	70
5.3 Future Research.....	71
References.....	73
Appendices.....	83
Appendix A: Additional Results.....	83
A1. Optimization of Electrospinning.....	83
A2. Dehydration of Phages.....	85
Appendix B: Permission to Reproduce.....	87

LIST OF TABLES

Table 2.1: Physical properties of PHB.....	19
Table 2.2: Process-related parameters for electrospinning.....	24
Table 2.3: Ambient parameters for electrospinning.....	24
Table 2.4: Solution-related parameters for electrospinning.....	25
Table 3.1: PHB substrates prepared in this study.....	28
Table 3.2: Composition of PBS solution.....	29
Table 4.1: Mass and thickness of each PHB substrate used in the study. All samples were squares of equal area (0.25 cm ²).....	44
Table 4.2 Bioluminescent reporter phages for the detection of <i>E. coli</i> O157: H7.....	65

LIST OF FIGURES

Figure 1.1: People infected with outbreak strain of <i>E. coli</i> O157:H7 in 2018: (a) state of residence (b) date of illness onset ¹² . Epidemiologic and traceback evidences demonstrated that the infections were linked to romaine lettuce from the Yuma growing region, Arizona.....	3
Figure 2.1: Structures of tailed phages ²⁶	10
Figure 2.2: Statistics of phages genera and species correspond to bacterial genera ²⁵	10
Figure 2.3: Schematic diagram of a biosensor comprised of 3 components: bioreceptors, transducers and data processors ²⁷	11
Figure 2.4: Chemical structure of PHB.....	19
Figure 2.5: Schematic of a basic electrospinning system. The polymer jet travels in a straight line within a short distance and then bends in whipping motion as a result of instability of the jet..	22
Figure 3.1: PHB substrates prepared in this study. (a).EB mat (1% w/v PHB in chloroform); (b) EF mat (5% w/v PHB in chloroform); (c) LCSC film (1% w/v PHB in chloroform); (d) HCSC film (5% w/v PHB in chloroform).....	29
Figure 3.2: PHB solutions at room temperature: 1% w/v (white lid) and 5 % w/v (green lid).....	30
Figure 3.3: Schematic of electrospinning system.....	31
Figure 3.4: Electrospinning setup in chemical hood.....	31
Figure 3.5: Close-up view of electrospinning setup.....	32
Figure 3.6: EB mat.....	34
Figure 3.7: EF mat.....	34
Figure 3.8: Phage immobilization of EF mat in a centrifuge tube containing 100 μ L of phage suspension at a titer of 2×10^8 pfu/mL.....	36
Figure 3.9: Electrospun samples prepared for WCA measurements. Triplicate are shown for two different conditions tested.....	38

Figure 3.10: Phage-immobilized PHB substrates mounted on studs for Helium Ion Microscopy.....	40
Figure 3.11: A phage immobilized EF mat (indicated by arrow) immersed in <i>E. coli</i> suspension.....	41
Figure 3.12: A 24-well plate containing phage immobilized PHB substrates and TSB media.....	43
Figure 4.1: Scanning electron microscopy of a,e) EB mats, b,f) EF mats, c,g)LSCS film and d,h) HSCS film.....	45
Figure 4.2: Water contact angle (WCA) measurements of PHB substrates.....	47
Figure 4.3: Number of phages loaded on substrates per surface, assuming no volume loss of phage lysate during overnight immobilization. Triplicates were performed for these experiments.....	49
Figure 4.4: Phages released from PHB substrates during washing. Average values and standard deviations are reported and were based on triplicate measurements.....	50
Figure 4.5: Imaging of phage particles immobilized on PHB substrates (EB mat, EF mat, LCSC film and HCSC film) using helium ion microscopy. Images are shown for each substrate, and for each substrate exposed to phages (phage-immobilized after 4 washing steps). Images were taken at 4 different locations of PHB substrates. Images with the most number of phages were presented.....	52
Figure 4.6: Fluorescent confocal microscopy images of PHB electrospun mats incubated with phage suspensions containing 10^9 PFU/ml. Imaging was made at the center (a, b) and edge (c, d) of the PHB control mats (a, c) and the PHB mats with phages (b, d). Phages, stained with SYBR green I, appear in green; PHB fibers appear in blue due to autofluorescence.....	54
Figure 4.7: Phage-immobilized PHB substrates (0.25 cm^2) were incubated with <i>E. coli</i> O157: H7 for 5 h. The results are presented with standard deviations from triplicates. Arrow indicates the time point where substrates were added to the culture.....	55

Figure 4.8: Detection of the presence of *E. coli* cells in a culture by PHB substrates with immobilized phage PPO1 modified to express Nanoluc, as measured by bioluminescence. Triplicate measurements were performed, and average values and standard deviations are shown (in some cases the size of the error bars is smaller than the data points). Control condition is the average measurement of 4 samples consisting of only PHB substrate (no phage), one for each type of PHB substrate.....56

Figure 4.9: Bioluminescence of phage-immobilized EF mats exposed to *E. coli* cultures at various cell counts. No pre-enrichment step was performed prior to incubation. Control is the substrate without *E. coli*. Results were obtained from triplicates and the error reported is based on standard deviations.....58

Figure 4.10: Bioluminescence of phage-immobilized electrospun PHB fiber swabs exposed for 1 min to pure TSB medium containing various cell counts of *E. coli* cultures, and incubated in TSB medium at 37°C. Control is the substrate without *E. coli*. Results were obtained from triplicates and the error reported is based on standard deviations.....60

Figure 4.11: Bioluminescence of phage-immobilized electrospun PHB fiber swabs exposed for 1 min to contaminated milk containing various cell counts of *E. coli* cultures, and incubated in TSB medium at 37°C. Control is the substrate without *E. coli*. Results were obtained from triplicates and the error reported is based on standard deviations.....60

NOMENCLATURE AND ABBREVIATIONS

Symbols

LD ₅₀	lethal dose, 50%
M _w	weight average molecular weight
p	probability value
T _g	glass transition temperature (°C)

Abbreviations

CDC	US centers for disease control and prevention
CFU	colony forming units
CNT	cationic carbon nanotubes
DNA	deoxyribonucleic acid
dsDNA	double-stranded deoxyribonucleic acid
<i>E. coli</i>	<i>escherichia coli</i>
EDC	1-ethyl-3-(3-(dimethylamino)propyl)carbodiimide hydrochloride
ELISA	enzyme-linked immunosorbent assay
FESEM	field emission scanning electron microscope
HIM	helium ion microscope
HUS	hemolytic uremic syndrome
<i>L. monocytogenes</i>	<i>listeria monocytogenes</i>
lux	luciferase
NLuc	nanoluc
OD ₆₀₀	optical density at 600nm
PBS	phosphate-buffered saline (PBS)
PCR	polymerase chain reaction

PDI	polydispersity index
PFU	plaque forming unit
pH	potential of hydrogen
PHA	polyhydroxyalkanoate
Phage	bacteriophage
PHB	polyhydroxybutyrate
PHBV	poly(3-hydroxybutyrate-co-3-hydroxyvalerate)
PLA	polylactic acid
PSPH	poly [5,5-dimethyl-3-(3'-triethoxysilylpropyl)-hydantoin]
SEM	scanning electron microscopy
STEC	shiga toxin <i>E. coli</i>
TSB	tryptic soy broth
UV	ultraviolet
WCA	water contact angle

1. Introduction

This study aims to design a fast, selective and cost-effective sensor to detect *Escherichia coli* O157:H7 in food products. This can be achieved via the immobilization of a modified bacteriophage (phage) expressing the reporter protein NanoLuc (Nluc) on a substrate fabricated from polyhydroxybutyrate (PHB), which is a biopolymer. To date, this approach of immobilizing phages on polymer substrates has been under-studied in the scientific community. This chapter introduces the context, summarizes the motivation and details the objectives for this work before providing an outline of this thesis and the chapters within it.

1.1. Background and Motivation

As human population grows, there is an insatiable need for more food products. With this increasing demand comes a need for improved food safety – a global concern aimed at reducing or eliminating contamination of food products¹. Unfortunately, despite the establishment of efficient food safety practices, it is still rare to find an individual who has not gone through an unpleasant moment linked to contaminated food in his or her lifetime.

Generally, contaminated food is defined as foods that are tainted or spoiled, containing bacteria, viruses, parasites or substances that eventually cause illnesses². Not only are these illnesses pervasive and expensive to treat, they also pose a threat to worldwide public health safety³. Cases of foodborne illnesses are increasing globally, particularly in developing countries due to lack of awareness in personal and food hygiene⁴. Increased trade, immigration and travel also facilitate transfer of dangerous contaminants and pathogens across borders. According to the US Center for Disease Control and Prevention (CDC), one out of every six people in the United States is infected with foodborne illnesses every year, this resulted in 128,000 hospitalizations and 3,000 deaths in 2011 alone⁵. In addition, an article published by the World Health Organization stated that, “at least 600 million people, or almost 1 in 10 worldwide, fall ill from contaminated food each year and 42,000 died, many of them were young children”⁶.

The most common pathogens that affect millions of people annually with severe and fatal outcomes are *Salmonella*, *Campylobacter*, *Listeria*, *Vibrio cholerae*, and enterohaemorrhagic *Escherichia coli*⁷. Amongst these pathogens, *E. coli* accounted for 41% of the microbiological contamination cases in 2014, based on data reported from the Department for Environment Food & Rural Affairs, United Kingdom⁸. Most types of *E. coli* are harmless and are actually a part of the microflora in a healthy human and animal intestinal tract. However, Shiga Toxin *E. coli* (STEC) produces toxins and causes disease. Infection by *E. coli* O157:H7, a STEC strain, is associated with undercooked meat, unpasteurized milk, raw fruits and vegetables. It is usually transmitted through contaminated water or food, or through physical contact with animals and humans. People of all ages can potentially be infected, however, elderly and young children have greater risk of developing hemolytic uremic syndrome (HUS), a life-threatening form of kidney failure.

In United States, *E. coli* O157:H7 is the most commonly found pathogenic *E. coli*. It is estimated that 265,000 STEC infections occur each year in the United States, 36% of these cases are attributed to *E. coli* O157:H7⁹. The first reported outbreak of *E. coli* O157:H7 in the United States occurred among fast-foods consumers where cases were associated with undercooked ground beef¹⁰. A more recent outbreak of *E. coli* O157:H7 spread over multiple states and was linked to contaminated romaine lettuce¹¹⁻¹². While the outbreak appeared to be over as of June 28, 2018, 210 people ended up being infected across 36 states (shown in Fig. 1.1) which led to 96 hospitalizations and 5 deaths¹².

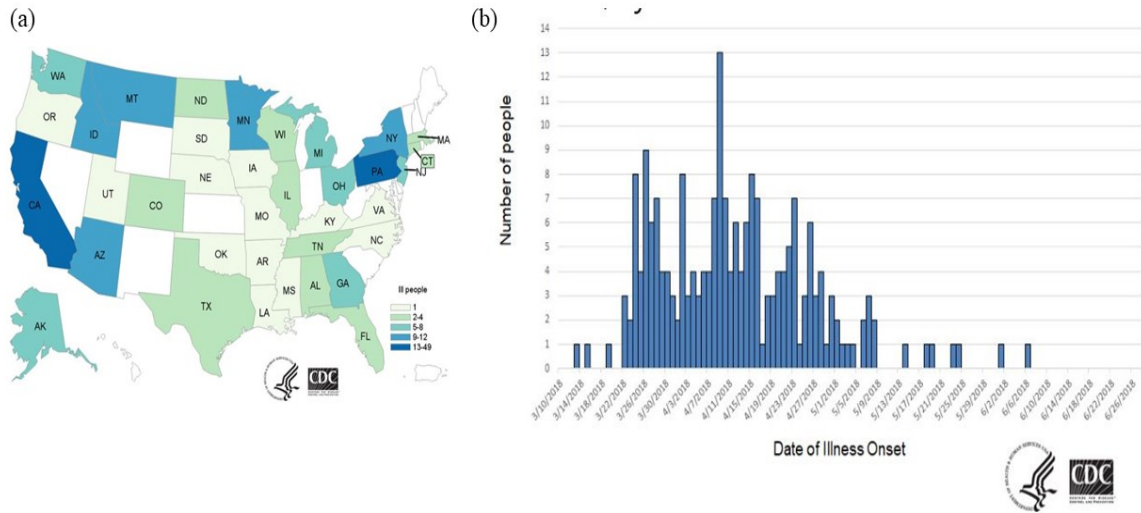


Figure 1.1: People infected with outbreak strain of *E. coli* O157:H7 in 2018: (a) state of residence (b) date of illness onset¹². Epidemiologic and traceback evidences demonstrated that the infections were linked to romaine lettuce from the Yuma growing region, Arizona. (Permission not required for use of public domain items)

In November 2018, another *E. coli* O157:H7 outbreak was linked to romaine lettuce, albeit not related to the lettuce-borne outbreak mentioned above as the DNA fingerprints of the *E. coli* strains differed¹³. This outbreak affected at least 50 people in both the United States and Canada¹³. In Canada, a total of 29 confirmed cases were investigated in Ontario (5), Quebec (20), New Brunswick (1), and British Columbia (3)¹³. Among them, 10 individuals were hospitalized and 2 individuals suffered from HUS¹³. The age of infected individuals ranged from 2 to 93 years old¹³.

Due the severity of the infection, outbreaks of *E. coli* O157:H7 in Canada have been carefully monitored and reported by the Public Health Agency of Canada. However, there is no current treatment to cure the infection¹⁴. Antibiotics have not been shown to alleviate symptoms, and therefore, are not recommended for the fear of increasing risk of serious complications¹⁴. Instead, supportive treatment, such as fluids to prevent dehydration and fatigue, is given to patients infected by *E. coli* O157:H7¹⁴. Patients who develop complications are likely hospitalized for intensive care, including dialysis and other specific therapies¹⁴. In addition, the origins of food

poisoning outbreaks are difficult to trace, owing to the complicated, often international, networks of food production and distribution¹⁵. Countries that act as distribution hubs of the food traffic are highly vulnerable¹⁵. Therefore, tracing and identifying the origins of foodborne outbreaks is anticipated to increase in complexity and impact, considering the current trend of increasing globalization.

Conventional *E. coli* detection methods rely on microbial cultures, polymerase chain reaction (PCR) and/or enzyme-linked immunosorbent assay (ELISA). These methods each have their inherent weaknesses, which include being time consuming or expensive given that they require skilled labor. In this work, an effective bacterial sensing method for the detection of *E. coli* O157:H7, namely reporter phage-based biosensor, addressing the above problems was investigated. Phages are bacteria-killing viruses that infect specific bacterial species or strains. Reporter phages are genetically modified phages that carry a foreign gene expressing a protein or enzyme that can be detected or monitored. In addition to detection, phages have been shown to effectively inhibit bacterial growth in some food products, making them of interest to be used in antimicrobial packaging. To implement phages in these applications, it is desirable to immobilize them on a substrate such as a polymer thin film. Immobilization of phages on PHB polymer with microstructures may enhance phage infectivity thus improving the overall efficiency of the biosensor.

1.2. Objectives of Study

The overall purpose of this research was to develop a biosensor device for detection of *E. coli* O157:H7. The biosensor was made through the immobilization of reporter PPO1 phage expressing the luminescent protein Nluc on PHB substrates. PHB is a biopolymer that has been proposed as food packaging material for short-lived plastic products where its biodegradability is a strong benefit¹⁶.

The objectives of this work include:

- a) To fabricate PHB substrate of various morphologies through electrospinning and solvent casting.
- b) To effectively immobilize Nluc reporter phage PPO1 on the polymer substrate and study its performance.
- c) To demonstrate potential use of immobilized phages on a PHB substrate as a biosensor for the detection of *E. coli* O157: H7 in food samples.
- d) To study the efficiency of immobilized phages on different PHB substrates.

1.3. Organization of the Thesis

The present thesis is organized as follows:

Chapter 2 introduces the underlying concepts involved in the development and application of the biosensor. This includes discussions on phages, reporter phages, phage immobilization, PHB and electrospinning. Chapter 3 describes the methodology used in preparation of the phage immobilized PHB substrates and the characterization of the resulting materials. In chapter 4, the performance of reporter phages immobilized on PHB substrates as biosensor is analyzed. Finally, chapter 5 presents the conclusion and significance of this research with emphasis on the key results. Recommendations for future work are also stated at the end of this chapter.

2. Literature Review

In this chapter, methods for the detection of *Escherichia coli* are discussed and phage-based biosensors are introduced as alternative diagnostic tools for *E. coli* detection. Next, an overview of biosensors and how phages are incorporated into biosensor platforms is presented. A specific type of reporter phage, expressing the enzyme luciferase, is explained. Also, the features and challenges of phage immobilization are noted. Finally, the characteristics of PHB and electrospinning as a processing method to achieve highly porous fibrous mats of PHB are reviewed.

2.1 *E. coli* Detection

E. coli is a Gram-negative bacteria found in the lower intestine of warm-blooded organisms, among other environments¹⁷. Most *E. coli* are harmless, however, strains such as Shiga toxin-producing *E. coli* O157:H7 can cause food poisoning and severe disease¹⁷. The presence of *E. coli* in ready-to-eat food can result from contamination by faecal matter and improper hygiene at processing facilities¹⁸. In many countries, drinking water quality is periodically monitored for *E. coli* to reduce risk of infection. The acceptable upper limits for *E. coli* fecal coliforms content are 200 colony forming units (CFU) per 100 ml and 35 CFU/100 ml for fresh surface water and marine water, respectively¹⁹. In Canada, based on the Hazard Analysis and Critical Control Points system, raw beef products should show no detectable level of *E. coli* O157²⁰. Despite various efforts to improve hygiene practices, this foodborne pathogen still poses high risks to the public health. The current methods of detecting *E. coli* O157:H7 are culture-based diagnostic protocols, immunological and polymerase chain reaction (PCR)-based techniques.

In the conventional culture-based method, target pathogens from food samples are incubated in specific liquid growth media for enrichment, followed by plating onto selective agar plates. Pure cultures are then isolated and undergo a series of tests (e.g. phenotypic and physiological) to confirm the results. Depending on the type of bacteria to be identified, the

incubation periods can vary from 48 to 72 hours²¹. It may take several days of repeated culture and confirmation steps to yield reliable results. Although this method is time consuming and labor intensive, colonies of bacteria produced by plating can be further analyzed for source tracking²¹. The detection of *E. coli* O157:H7, following the standard protocol from the US Department of Agriculture Food Safety and Inspection Service, requires enrichment of meat products in a selective broth medium and testing of enrichments using a screening assay, prior to plating onto a selective agar medium²². Following this, colonies are tested biochemically and serologically to confirm the presence of Shiga toxin genes²².

The immunological method utilizes antibodies to detect specific antigens, other antibodies and proteins in samples. At present, enzyme-linked immunosorbent assay (ELISA) is the most established immunological technique for the detection of pathogens. The immuno-based techniques can identify pathogens based on the antigenic determinants expressed on the bacteria cell surface, such as lipopolysaccharides, membrane proteins, and extracellular organelles including flagellae and fimbriae. There are five steps in preparing ELISA. First, a microtiter plate well is coated with antigen. Unbound sites are blocked to avoid false-positive result. Then, antibodies are added to the wells before anti-antibodies conjugated to an enzyme are added. Finally, substrate is added to react with the enzyme to produce colometric signals, indicating a positive reaction. Some examples of the enzymes used in ELISA are alkaline phosphatase, horseradish peroxidase and urease. ELISA is a much faster detection method than the conventional culture-based technique. A detectable signal can be generated within 5 h²³. However, the tests are laborious, expensive and prone to yield false positive results²³.

Polymerase chain reaction is a molecular biology method to amplify a specific segment of DNA into thousands to million copies of that particular DNA segment. The process of PCR assay can be separated into 3 categorizes: pre-PCR processing, PCR reaction, and post-processing.

Pre-PCR processing includes sampling and sample preparation. The main reasons of pre-PCR processing are to exclude PCR-inhibitory substances that may reduce sensitivity of the assay, to increase the concentration of target organism up to practical operating range, and to produce homogenous samples for repeatability. Depending on the type of food sample, different sample preparation methods are employed. These are categorized as biochemical, immunological, physical and physiological methods.

In PCR, samples are processed through repeated heating and cooling to denature, anneal and extend DNA strands. The first step of thermal cycling involves denaturing a double-stranded DNA (dsDNA) segment into two single-stranded ones and produce the template for further amplification. In the second step, the designed primer, which matches a section of the DNA template sequence, is annealed to the single-stranded DNA and begins to form dsDNA throughout the extension step. Then, the amount of DNA is doubled in the extension step. These steps are repeated for the specific DNA fragment to be exponentially amplified.

Post-processing takes place once the amplification step is finished. The PCR products are compared with nucleotide fragments of known sizes in a separating gel. Electrical current is applied to the gel, separating the nucleotide sequences into bands based on their molecular sizes. The PCR products can also be analyzed through sequencing to identify the bacterial strain from which they originate.

In *E. coli* O157:H7 detection, PCR analysis has been used to identify the presence of Stx1 and Stx2 genes, which are specific to the pathogen²¹. With PCR, the analysis time can be shortened and detailed genetic information on the pathogen virulence, resistance against antibiotics and epidemiology can be obtained²¹. Nonetheless, PCR has one major drawback which is its lack of ability to distinguish between live and dead cells.

2.2 Phage-based Biosensors

The methods currently used for the detection of *E. coli* are often laborious and time consuming²¹. As an alternative to conventional microbiological methods, novel biosensors involving phages as recognition elements are being developed.

Phages are known as natural predators of bacteria. These “bacteria-eating” viruses are ubiquitous and can be found wherever bacteria survive²⁴. It is estimated that there are more than 10^{31} phages on the earth, which exceeds every other population of organisms, including bacteria²⁴.

Phages can be classified based on their genome and morphology. Tailed phages from Myoviridae, Siphoviridae and Podoviridae family group (Fig. 2.1) form the most abundant biological entity on earth. They have a dsDNA genome enclosed in a polyhedral head, also known as capsid. The tail fibers are used to identify the receptor of the host cells to enable genome entry into the bacterium following adsorption. Fig 2.2 provides an overview of the prevalence of phage genera and species identified to date and that act on different bacterial genera²⁵.

The first stage in virus-host recognition is adsorption of phage to a receptor on the host cell surface. The specificity of this interaction is dependent on the nature and structure of receptors on the bacterial cell surface. The receptors may be proteins localized in the membrane and lipopolysaccharide of the bacteria, lipopolysaccharide membrane itself, bacterial fli or flagella and et cetera. The nature of phage receptor is different and defined by composition of host cell wall and surface structures.

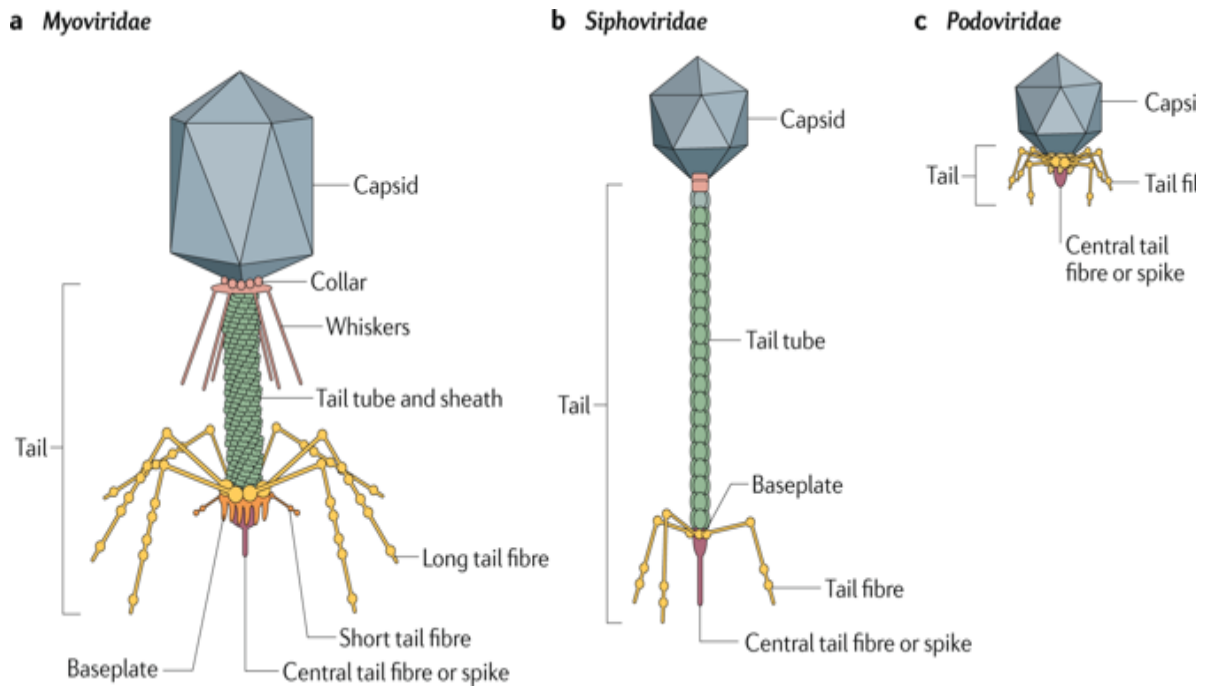


Figure 2.1: Structures of tailed phages²⁶. Used with permission.

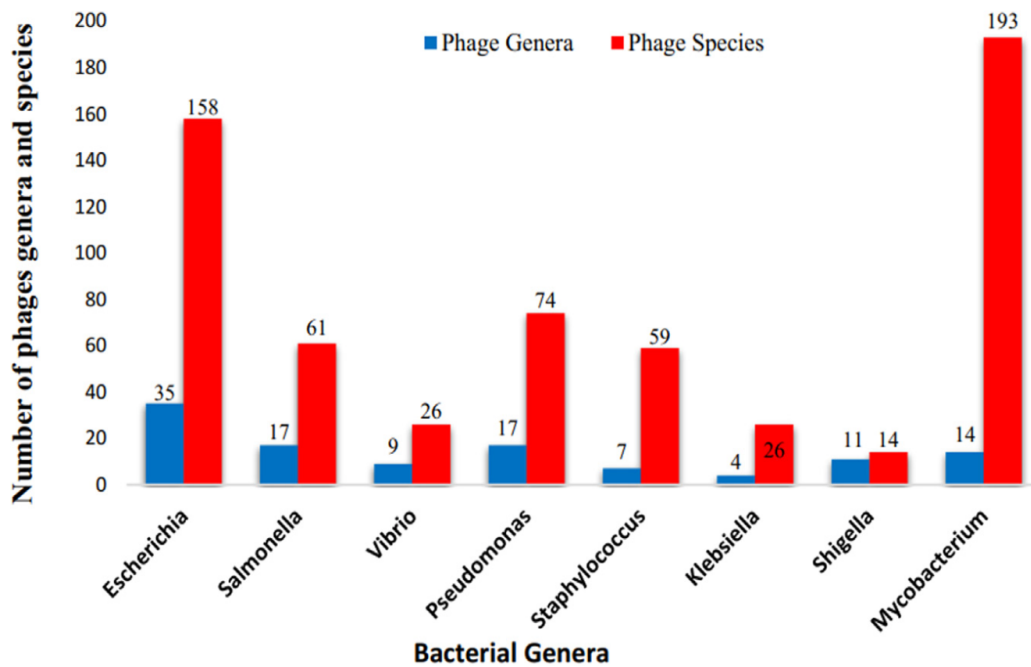


Figure 2.2: Statistics of phages genera and species correspond to bacterial genera²⁵. Used with permission.

A biosensor is an analytical device which converts a physical or biological event into measurable signal. It is typically made up of several components, including bioreceptor, transducer and signal processor (Fig. 2.3). Bioreceptors serve as biological probes to interact with a specific analyte of interest. The transducer then converts the recognition event into a measurable signal. In this context, phages are used directly or as an assembly with other components to act as a sensing layer where they infect target cells and serve as a specific bioreceptor.

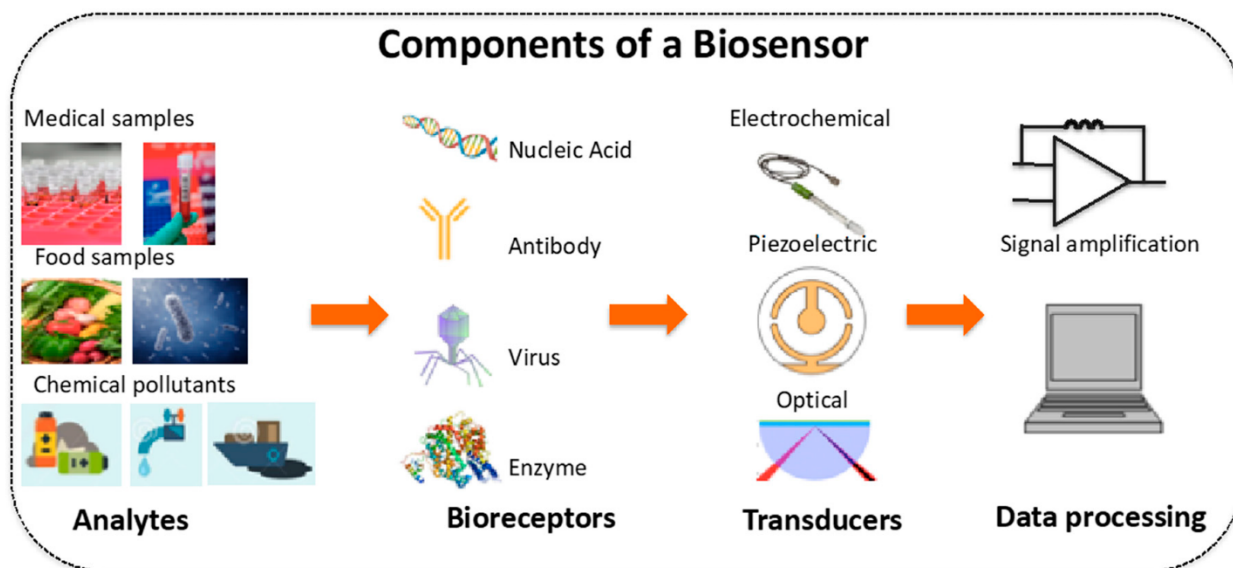


Figure 2.3: Schematic diagram of a biosensor comprised of 3 components: bioreceptors, transducers and data processors²⁷. Used with permission.

The use of phages as detection probes offers several advantages for bacterial sensing including: (1) High specificity to host bacterium²⁵. Phages infect their hosts through recognizing receptors on the bacterial cell wall. They are very specific, sometimes even targeting a single strain of bacteria. (2) The capability to amplify upon infection. The burst size of phages (amount of phage released per host cell infected) can reach the thousands of progeny²⁵. This means that the amount of elements enabling recognition of the pathogenic bacteria can increase throughout detection. (3) High tolerance against environmental stresses. As compared to antibodies, phage particles are more stable in organic solvents, at high temperature and over a wider range of pH

values. (4) Benign to human and animals²⁵. Due to their high specificity, phages only infect their host cells. In addition, degradation of phages by antibodies or immune system do not produce toxic by-products²⁸. It has been show that the low immunogenicity of phages does not represent significant risks for patients²⁸. Therefore, phage therapy is relatively benign when compared to antibiotic therapies²⁸. (5) Ability to distinguish live and dead cells. Phages cannot propagate without their host. Therefore, the phage detection method that relies on infection of viable cells to produce measurable signals only works when live cells are present. (6) Simple and cheap mass production. The production of phages is considered easier and less costly compared to other biological bioreceptors (e.g. antibodies).

2.3 Luciferase Reporter Phages

Reporter phages are genetically modified phages that contain a heterogenous gene within their genome²⁹. Several genes, for examples, alkaline phosphatase, green fluorescent protein, beta-galactosidase and bacterial luciferases have been used as reporter genes for detection of different pathogenic bacteria²⁹. Compared to other phage-based sensors, reporter phages have the advantage of generating measurable signals upon infecting their target pathogen, thereby functioning as both bioreceptor and biotransducer components. During the phage infection, phages inject their genome, including the reporter genes, into the bacteria cells. These reporter genes are expressed by the bacteria, which leads to active production of reporter protein or enzyme, transforming the bacteria into biomarkers allowing detection. The amount of expressed protein or enzyme can be tied to the quantity/number of infected bacteria within the sample²⁹.

Among the reporter genes investigated so far, luciferase is more commonly used in reporter phages because of its greater sensitivity³⁰. The luciferase reporter gene assay produces measurable signals in bioluminescence, which is a form of light emission from living organisms through chemical reactions. It is usually an enzyme-catalyzed process, where the substrate, luciferin, meets the enzyme partner, luciferase, with the addition of energy and atmospheric

oxygen, produces oxyluciferin, emitting photons of light³¹. Luciferases can be found in organisms such as bacteria, algae, jellyfish, shrimp, squid and fireflies³¹. The full luciferase gene cassette consists of 5 genes, *luxA*, *luxB*, *luxC*, *luxD*, and *luxE*³¹. Sometimes, a bioreporter does not contain the full *lux* gene cassette. In that case, the bioreporter requires addition of substrates to generate bioluminescence signals³². Nanoluc (Nluc) luciferase is the newest commercially available luciferase enzyme developed by Promega³³. NLuc is of relative small size (19kDa), facilitating gene insertion into the phage genome and capsid³³. Other than that, the system is able to generate greater signals and possess higher thermal stability than other luciferases²⁹.

Luciferase is 10- to 1000-fold more sensitive than green fluorescent protein (e.g, another protein commonly used in bioimaging), based on excitation of fluorescent proteins at a specific light wavelength and detection of light emission at another wavelength with a charge-coupled camera³³. Also, given that food materials generally do not bioluminescent, a high signal to noise ratio can be obtained²⁹.

The first luciferase reporter phage was constructed by Ulitzur and coworkers on phage lambda, termed L28³⁴. The *lux AB* reporter phage could detect as few as 10 *E. coli* cells/ml in milk within 1 hour³⁴. Kim and coworkers, introduced the *lux CDABE* bioluminescence operon into the genome of the *Salmonella* temperate phage SPC32H³⁵. In pure cultures, the reporter phage could detect 20 CFU/ml of *Salmonella Typhimurium* within 2 hours³⁵.

Ripp et al. had designed a reporter phage PPO1 based on *luxI/R* quorum sensing and a *lux CDABE* operon³⁶. The reporter phage detected original inoculum of 1 CFU/ml in 16 hours assay time after a 6 hours incubation³⁶. A NanoLuc reporter phage assay was developed by Zhang et al. in lysogenic phage phiV10 for detection of *E. coli* O157:H7³⁷. The recombinant phage was able to detect low quantity of *E. coli* cells, 5-6 cells within 7-9 hours in pure culture and ground beef enrichment with small amount of reporter phage (10^2 - 10^4 PFU/ml)³⁷. In 2018, Hinkley et al.

published the construction of reporter phage T7_{NLC} using NLuc fused with carbohydrate binding module CBM2a to detect *E. coli* cells in drinking water³⁸. The phage featured a detection limit of less than 10 CFU/ml in 3 hour of assay time aided with 1 hour of pre-enrichment³⁸.

Despite its promising features, the bioluminescent reporter phage assay has a drawback: there is transient emission of bioluminescence after adding the luciferin substrate²⁹. The signal half-life of the NLuc system is approximately 2 hours³⁰. Additionally, bioluminescence measurements are usually performed on multi-plates with phage-infected bacteria in liquid samples²⁹. However, such measurements may be relatively expensive to perform with a luminescence reader, on par with other high-throughput screening methods²⁹. Immobilized phages may offer an easier or cheaper alternative with a lab on a chip approach²⁹. In addition, Polaroid film could offer an inexpensive alternative to luminometer to lower the cost of the diagnostic tool. Hazbon et al. attempted to build a Bronx box to detect luminescence signals from reporter phages³⁹. The Bronx box is an enclosed box, where a Polaroid film cassette is placed over a micro-plate containing the luciferase reporter phages and infected bacteria cultures³⁹. The film was exposed overnight and light signals were obtained as photographic results³⁹.

2.4 Phage Immobilization

As discussed in the previous sections, phages can be employed as specific recognition elements to detect or capture target analytes. In addition, phages can be incorporated to surfaces to render them bioactive. Numerous approaches are reported to effectively immobilize phages on a solid substrate.

The simplest approach is through physisorption. Nanduri demonstrated that phages can be immobilized on the surface of a quartz crystal microbalance through physical adsorption and remained active after immobilization⁴⁰. However, physisorption is a non-specific binding process and phages can dissociate from the surface.

Alternatively, chemisorption, which involves the formation of chemical bonds, offers stronger bonding on substrates. Chemical bonding can be done through protein conjugation (e.g. biotin-streptavidin interactions⁴¹) or various covalent bond chemistry targeting the endogenous amino acids on the envelope of phages to build the covalent bonding between the phages and the substrates⁴³⁻⁵². However, some of the chemicals required for these approaches may damage phage integrity or decrease their infectivity due to harsh reaction with the phage proteins⁵³. For example, Wang et al. studied immobilization of phage T4 on polymer and tested different combinations of chemicals to promote covalent bonding with the substrate⁵⁴. They found that phages immobilized on plasma-treated polymer without any chemical bonding retained the highest infectivity towards the host cells compared to phages immobilized with other methods⁵⁴. It was suggested that the chemical reagent 1-ethyl-3-(3-(dimethylamino)propyl)carbodiimide hydrochloride (EDC), used to cross link phages on polymers, may damage phage integrity during the reaction. EDC is known to be harmful for certain cell types and may also cause severe eye damage⁵⁵.

2.4.1 Challenges in Phage Immobilization

A few challenges must be addressed in designing phage-associated bioactive surfaces. These include the activity, orientation and packing density of phages, which are critical in determining the performance of the resulting materials.

It is crucial that immobilized phages retain their infectivity, regardless of the immobilization methods. Even though phages are more robust than many other biorecognition elements, such as enzymes and antibodies, they can become inactivated upon exposure to harsh conditions, which include reactive chemicals, pH, UV light etc. Puapermpoonsiri et al. attempted to create microspheres containing phages for pulmonary delivery⁵⁶. Their result showed that the encapsulated phages partially lost their infectivity. Dichloromethane was reported to be the root cause as it is known to denature proteins⁵⁶.

The orientation of immobilized phage particles is particularly important due to the geometric structure of many phages and the phage-host recognition mechanism: the recognition and induction of infection is often done by the interaction of the tip of the phage tail (tail fibers, baseplate, etc.) with the host⁵⁷. While free phages diffuse and easily change orientation, allowing for the recognition of target host cells, immobilized phages do not have the freedom to do so. In fact, bacterial cells have to diffuse to the immobilized phage layer and phages could only infect the cells if their tail and tail fibers are properly oriented and free to move. Therefore, the optimum condition for immobilized phages is to orient them in such a way that the movement of the tail and, when appropriate, tail fibers are not hampered⁵⁷.

Furthermore, most phages have charges on them, making many phage particles similar to dipoles. The capsid of tailed phages is generally negatively charged while the tail is slightly positive charged⁵³. Scientists have turned to electrostatic binding to anchor phages on substrates in order to optimize the orientation of immobilized phages. Zhou and coworkers oriented T2 phages on cationic carbon nanotubes (CNT) through electric field manipulation and achieved detection limit of 10^3 CFU/ml for their biosensor⁵⁸.

Once a method is established to properly align phages on a substrate, efficiency of the bioactive surface may be further improved by increasing the packing density of phages. Naidoo et al. suggested that above a threshold surface density of immobilized phages, bacterial capture efficiency started to decrease as a result of entanglement of phage tail fibers, impeding interactions with the host bacteria⁵⁹. Regarding this issue, Richter determined that the maximum coverage of phage T4 was 19 phages/ μm^2 with randomly oriented phages⁶⁰. However, by properly aligning phages with alternating electric field, the researchers were able to attach a dense layer of oriented phages on a surface, improving the packing density of phages up to 100 phages/ μm^2 . The optimized performance of the surface with oriented T4 receptors had 64-fold higher sensitivity than the surface with randomly oriented counterparts⁶⁰.

2.4.2 Application of Phage Immobilization

Phage immobilization imparts additional functionality to a surface, which enables applications in biosensors, food packaging and medical devices.

In biosensors, reporter phages have been immobilized on substrates to serve as both bioreceptors (to recognize particular analyte of interest²⁷) and transducers (to convert biological activity into a measurable signal²⁷). For example, some genetically modified phages generate easy to read colorimetric signals upon encountering specific pathogens; thereby eliminating the need of sophisticated electronic instruments to generate signals and aligning with the idea of lab-on-chip systems. Lab-on-chip systems make biosensors portable and facilitate rapid point-of-care detection, not to mention creating savings from reduction of trained lab workforce and specialist equipment.

Examples include phage T7 modified to express beta-galactosidase and immobilized on magnetic beads as created by Chen et al.⁶¹. Beta-galactosidase is released upon phage-mediated cell lysis and can be detected by adding red-beta-d-galactopyranoside, a colorimetric substrate that changes color in the presence of beta-galactosidase. The colorimetric signal can be determined through visual observation and allow for rapid detection of *E. coli* in resource-limited environment.

Paper diagnostics and dip-stick assays have also been reported in scientific literature. Jabrane et al. deposited phages onto paper surfaces with a pre-coat layer of cationic polymer to immobilise phages through electrostatic binding for detection of *E. coli*⁶². A rapid and ultrasensitive phage-based dipstick assay has also been developed by Anany et al., targeting *E. coli* O157:H7, *E. coli* O45:H2, and *Salmonella* Newport in spinach, ground beef and chicken⁶³. In this application, phages were immobilized on paper through piezoelectric inkjet printing. The paper assay was combined with quantitative real-time PCR to determine if DNA associated with

the target bacteria was present in broth and food samples. The limit of detection was found to be 10-50 CFU/ml in a total assay time of 8 hours⁶³.

Phages have also been attached to food packaging material to impart antimicrobial properties to the surface. Phages offer several desirable attributes as food antimicrobials. Firstly, they target pathogenic bacteria in food without disturbing the food quality. Secondly, phage biocontrol is an environmentally friendly antimicrobial intervention, considering the abundance of phages in environment. Thirdly, compared to free phage particles suspended in liquid lysate, immobilized phage particles only release free phages into the food when the pathogens of interest are present⁶⁴. This could alleviate consumer concerns regarding addition of viruses to food products.

One example of immobilized phages used as antimicrobial food packaging was demonstrated by Anany et al⁶⁵. The phage cocktails were immobilized on cellulose membranes to control *L. monocytogenes* and *E. coli* O157:H7⁶⁵. The authors conducted the study by applying the immobilized phage membranes on ready-to-eat turkey and ground beef under different storage conditions⁶⁵. They observed 1.5 log₁₀ reduction of *L. monocytogenes* on the turkey within 15 days and 1.0 log₁₀ reduction of *E. coli* O157:H7 in ground beef within 6 days, under aerobic conditions⁶⁵.

Some phages have been used towards therapeutic applications to treat bacterial infections. In Georgia, Poland and Russia, phage therapy is used to treat bacterial infections that do not respond to conventional antibiotics. For example, phages are used to suppress pathogenic bacteria directly at the site of a wound. However, phages in liquid preparation applied through dressings require frequent changes of the dressings to retain high local concentration of phages at the wound, which dramatically increases in-patient cost. To solve this problem, phages were immobilized on polymeric wound dressings so that phage particles could be released slowly and gradually over a period of time in the presence of pathogens⁶⁶.

2.5 Poly-3-hydroxybutyrate

2.5.1 Introduction to Poly-3-hydroxybutyrate

Poly-3-hydroxybutyrate (PHB) is a bio-polymer from the polyhydroxyalkanoate (PHA) polyester family. Its monomer, 3-hydroxybutyrate, has 3 carbon atoms as backbone and includes a methyl group, an alcohol group and a carboxylic acid group. The presence of the methyl group imparts hydrophobic characteristics to the polymer. The chemical structure and physical properties of PHB are displayed in Fig 2.4 and Table 2.1, respectively.

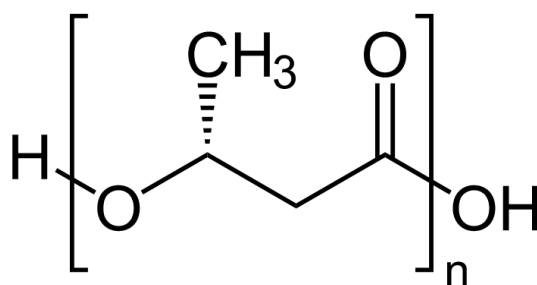


Figure 2.4: Chemical structure of PHB

Table 2.1: Physical properties of PHB⁶⁷.

Property	
Molecular weight (Da)	5 x10 ⁵
Glass transition temperature (°C)	15
Density (g/cm ³)	1.25
Crystallinity (%)	70
Young's modulus (GPa)	2.5-3.5
Tensile strength (MPa)	35-40
Extension to break (%)	5-7

Industrial production of PHB is typically done by microbial synthesis⁶⁷. Approximately 300 different microorganisms have been shown to be able to synthesize PHB⁶⁷. In most cases, a bacterium first consumes a carbon source and produces PHB in the form of granules as a reserve of energy to be metabolized when common energy sources are absent⁶⁸. Therefore, on one side, PHB can be completely biosynthesized and, on the other, completely catabolized to carbon dioxide and water, making it an attractive biodegradable material⁶⁸. Moreover, unlike other bioplastics, such as polylactic acid, which effectively break down only under composting condition greater than 55°C, degradation of PHB is possible under common environmental conditions, even in natural water environment^{69,70}. As an example, significant PHB film biodegradation, with mass losses of 11% within 14 days, was shown with the bacterial strain *Marinobacter algicola* under simulated marine environments at 30°C⁷¹.

Another desirable characteristic of PHB is the biocompatibility of the material, with PHB shown to be present in human bloodstream and its degradation product, 3-hydroxybutyric acid, being a common metabolite in organisms⁷². In fact, the dose of PHB necessary to achieve a decrease of 50% of a mammalian test population– its LD₅₀ – was found to be greater than 5000 mg/kg⁶⁹. Therefore, it can be considered completely nontoxic to mammals.

Due to its biodegradability and biocompatibility, PHB presents great potential in many applications related to the medical, pharmacological and packaging areas. For examples, PHB can be made into absorbable internal sutures, wound dressings, and tissue scaffolding for bone regeneration, to name just a few⁷³. In the pharmacological field, PHB can be used in thermogels for controlled-release drug delivery⁷³. PHB has been proposed as food packaging material for short-lived plastic products where biodegradability is a strong benefit⁷⁴. Studies have shown the polymer has good oxygen, water vapour, fat and odor barrier properties, which makes it suitable for storage of many liquids, acids and fatty food products⁶⁹. PHB's potential to replace petroleum-based plastics represent a significant step towards achieving a more sustainable

packaging industry, since it was found that food packaging waste comprises approximately one-third of all Canadian household waste⁷⁵.

As a thermoplastic, PHB can be melted and molded into many products suitable for consumer use⁶⁷. Some of the common processing methods used for PHB processing are extrusion and injection molding, where the former is commonly used for fibers, thin films, cast sheets and the latter for products like bottles and packages^{76,77}. However, despite its superior properties, the following challenges limit its widespread application in consumer products: (1) physical aging effects occur due to secondary crystallization making the polymer brittle over time, (2) low elongation at break due to slow crystallization rate promoting large spherulites in the structures, (3) narrow thermal processing window, where PHB degrades around 170-200 °C, and (4) high production cost due to low productivity of microbial synthesis, high costs of downstream processing and separation of PHB from cellular biomass^{72,73}.

2.6 Electrospinning of PHB

The properties of PHB, such as its biodegradability and biocompatibility, make this material a very strong candidate in food sensor applications. One key parameter governing the performance of many sensors is the surface area of the sensing element. In the biosensor system, as the surface area of the sensing probe increases, the probability of an encounter between the biorecognition elements distributed on the surface and the analyte of interest also increases, improving the sensitivity (as seen in many nanostructured sensor applications⁷⁸⁻⁸³). Hence, processing methods that enable a greater surface to volume ratio can be beneficial in many cases. Electrospinning is a well-established technique to fabricate nanostructured fiber mats under high applied voltage. In electrospinning, PHB fibers of micro- to nanometer-scale produce mats with high specific surface area and high porosity. These mats of high surface area enhance the interaction between the analyte and bioreceptor, making electrospun nanomaterials highly attractive as ultrasensitive sensors.

2.6.1 Introduction to Electrospinning

Electrospinning is a process to produce polymeric mats of submicron fibers under an applied electric field. Its underlying principle was discovered by William Gilbert over 375 years ago, when he noticed a cone tip formed on a drop of water while an electrically charged rubber amber was held close by the droplet⁸⁴. Electrospinning was further studied by Bose et al. in aerosol generated under electrical potential⁸⁵. Lord Rayleigh then investigated the surface tension of droplet detachment from different fluids⁸⁵. Although electrospinning has been around for a while, it mostly gained in popularity in the last three decades as electrospun nanofibers demonstrated superiority in nanotechnology and other related field⁸⁵.

A basic electrospinning system consists of a syringe pump, polymer melt/solution loaded on a syringe, a high voltage power supply and a grounded collector plate. A simple schematic is shown in Figure 2.5.

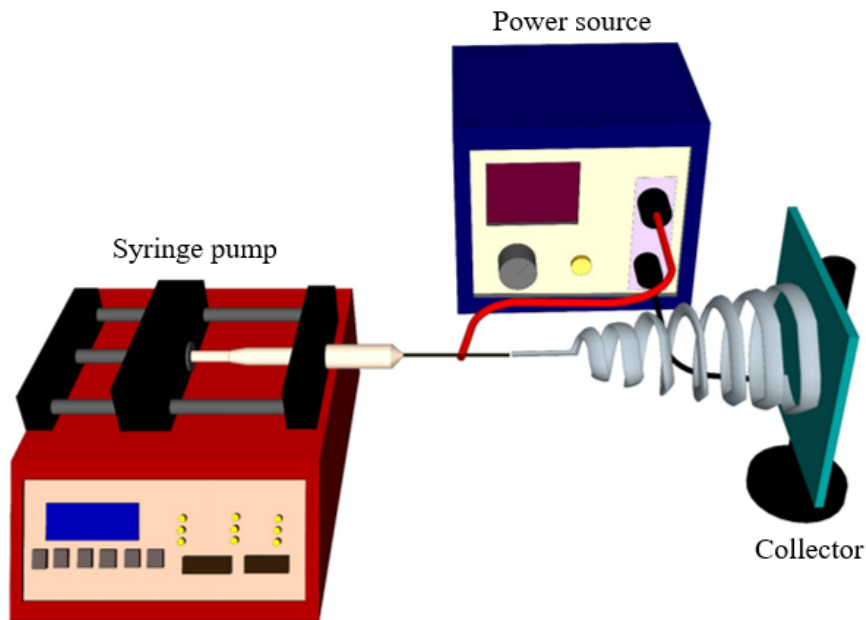


Figure 2.5: Schematic of a basic electrospinning system. The polymer jet travels in a straight line within a short distance and then bends in whipping motion as a result of instability of the jet.

In the process of electrospinning, a polymer solution, preferably with high conductivity, is filled in a syringe and subjected to high voltage (usually in the kV range) to provide sufficient electrical force to overcome surface tension of the solution, allowing continuous flow of liquid to be drawn out from the nozzle⁸⁶. As the solution is charged under an electric field, charge accumulates to a point where the repulsive force of the charges is equal to the surface tension of the polymer solution at the nozzle. At this point, a droplet of conical shape, known as a Taylor cone, forms at the nozzle. With increasing electrical field, the repulsive electrostatic force eventually overcomes the surface tension, a small liquid jet then forms from the tip of the Taylor cone. The polymer jet first travels in a straight line at a short distance, then starts to experience instability due to which it turns and bends in a whipping motion. This whipping motion causes the polymer jet to travel a longer path towards the collector plate, elongating the fiber and evaporating the solvent from the polymer jet, leaving dry polymeric strands of fiber deposited on the grounded plate⁸⁷.

Electrospinning is a simple process that can be done with a small laboratory setup⁸⁴. However, many parameters affect the final features of the resulting material, including the fiber diameter and size uniformity, and the material porosity. These parameters can be classified into three categories that affect the morphology of electrospun fibers: process-related parameters (applied voltage, flow rate and working distance; Table 2.2), ambient parameters (such as temperature, humidity and airflow; Table 2.3), and solution-related parameters (polymer concentration, polymer molecular weight, solution viscosity, solution surface tension, solvent conductivity, solvent volatility; Table 2.4). Bear in mind that these parameters are interrelated and their influence can vary. Successful electrospinning requires the combined optimization of these various parameters.

Table 2.2: Process-related parameters for electrospinning

Variable	Influence on diameter and morphology of fiber mats
I. Applied voltage	Applied voltage needs to overcome the threshold voltage to initiate electrospinning ⁸⁸ . As voltage is increased, fiber diameter initially decreases then increases ⁸⁵ .
II. Flow rate	At optimal flow rates, the polymer solution has sufficient cohesive forces to sustain a stable charge jet where a stable Taylor cone forms, producing the narrowest fibers possible ^{85,88} . At high flow rates, insufficient drying may occur due to limited time for solvent evaporation, resulting in thicker fibers, possibly with bead defects and/or flattened ribbon structures ⁸⁹ . At low flow rates, the Taylor cone is not stable and gradually reduces to form a fiber within the nozzle tip ⁹⁰ .
III. Working Distance	At the ideal working distance (usually around 10-20 cm), the applied voltage is in the optimal range where a stable charged jet can be formed and experience whipping to elongate before reaching the collector ⁹¹ . Shorter working distances leads to insufficient solvent evaporation ⁸⁴ . Increasing working distance from Taylor cone results in smaller fiber diameter ⁸⁵ .

Table 2.3: Ambient parameters for electrospinning

Variable	Influence on diameter and morphology of fiber mats
I. Temperature	Temperature affects the viscosity of the polymer solution as well as the evaporation of the solvent. High temperature increases the evaporation rate, leading to thicker fibers ⁸⁴ . However, as the viscosity decreases with increased temperature, the formation of thinner fibers is also possible, depending on the nature of polymer ⁸⁴ .
II. Humidity	Ambient humidity is important because it controls the solidification of the charged jet ⁸⁸ . Low relative humidity drives evaporation, resulting in thicker fibers. High moisture prohibits evaporation and imprints micro- and nanoscale pores on the surface of fibers ⁸⁴ .
III. Airflow	Airflow around the electrospinning setup controls the flight speed of the polymer jet ⁹² . High airflow encourages solvent evaporation, leading to higher fiber diameter ⁸⁴ .

Table 2.4: Solution-related parameters for electrospinning

Variable	Influence on diameter and morphology of fiber mats
I. Polymer Concentration	Polymer concentration contributes to fiber diameter through a power law relationship, with an exponent value of 0.5 ⁹³ . At the optimal concentration, polymer chains overlap during the stretching of the charged jet, resulting in the formation of smooth, beadless fibers. At low concentration, surface tension dominates the system, resulting in electrospayed beads or beaded fibers ⁹⁴ . Fiber diameter tends to increase with increasing concentration, however, in extreme cases, helix-shaped micron-scale ribbons have been observed ⁹⁵ .
II. Molecular Weight	Similar to the optimal polymer concentration, using ideal molecular weight of the polymer facilitates polymer entanglement, results in smooth fibers. If the molecular weight is low, bead-like structures are produced ⁸⁵ . On the other hand, if the molecular weight is too high, electrospinning is either not possible or results in fibers with large diameter ⁸⁵ .
III. Solution Viscosity	Viscosity depends on molecular weight and concentration of the polymer. It is important because it influences the formation of polymer jet when charges are applied to the solution. Ideal viscosity results in smooth fibers. Low viscosity polymer solutions form fine droplets with incomplete drying as surface tension dominates the system ⁸⁵ . At higher viscosity, formation of beads transition from spherical to spindle-like to smooth fibers ⁸⁸ .
IV. Surface Tension	Surface tension determines the cohesive forces between the molecules. Therefore, solutions with optimal surface tension experience stable repulsive forces from the charged solution and results in smooth fibers. Solutions with low surface tension and high viscosity form smooth fibers ⁹⁶ . Solution with high surface tension pose difficulties for the applied voltage to overcome the cohesive forces between the polymer molecules; in this case, electrospaying results in beaded fibers ⁹⁷ .
V. Solution Conductivity	The conductivity of the solution affects the charge-carrying capacity of the polymer solution, thus it influences the surface charge density of the polymer jet and the formation of Taylor cone ^{85,88} . Solutions with low conductivity have no charge on the surface of droplets to form a Taylor cone. Therefore, electrospinning will not occur ⁸⁸ . A highly conductive solution carries more charges and thus experiences stronger tensile force under electric field, decreasing fiber diameter ⁸⁵ . The addition of ionic salts decreases fiber diameter as well ⁸⁵ .
VI. Solvent Volatility	The choice of solvent affects the drying of fibers due to different evaporation rates. Insufficient drying results in ribbon-like fibers that may attach to the needle mid-air ⁹⁸ . Solvents with high volatility tend to cause the drying of polymer jet at the nozzle ⁸⁸ .

2.6.2 Literature Review of Electrospun PHB

There are many references in literature which highlight the relevance of electrospun PHB in biomedical applications. Electrospun fiber mats are used in tissue engineering, food packing and biosensing applications.

Sombatmankhong et al. studied electrospun fiber mats of PHB, Poly(3-hydroxybutyrate-co-3-hydroxyvalerate) (PHBV) and their blends as potential mammalian cells scaffold⁹⁴. The average diameter of the pure and blend fibers were approximately 2.3 and 4.0 μm . The electrospun membranes were more hydrophobic and possessed greater tensile strength than films produced through solvent casting⁹⁴. To test the potential of electrospun membranes as tissue scaffolds, the researchers conducted a cytotoxicity test with mouse fibroblasts. Their results indicated no threat to the cells.

Chan et al. synthesized a pectin-PHB copolymer via solventless ring-opening polymerization for retinal tissue engineering⁹⁹. The copolymer was blended and electrospun to produce nanofibers that were finer and less hydrophobic relative to pure PHB; it was also found to be soluble in organic solvents. The use of PHB provides mechanical support to the scaffolding structure while being biocompatible to the retinal cells. The biocompatibility and capacity of the fiber mats to support the proliferation and growth of seeded human retinal pigmented epithelium cells were reported, demonstrating the potential of this material as a scaffold for tissue engineering.

An antibacterial fibrous membrane has been fabricated based on a mixed solution of PHB and *N*-halamine compounds poly [5,5- dimethyl-3-(3'-triethoxysilylpropyl)hydantoin] (PSPH). The electrospun mat was then chlorinated in bleach to produce the antimicrobial material¹⁰⁰. The biocidal efficacy of the fabricated membranes was evaluated against both Gram-positive and Gram-negative bacteria. The chlorinated fibrous membranes could inactivate 92.10 % of *Staphylococcus aureus* cells and 85.04 % of *E. coli* O157: H7 cells within 30 min of contact time.

Finally, electrospun PHB has also been used in biosensing. Hosseini et al. coated polymethacrylate on electrospun PHB fibers to immobilize dengue antibody for dengue detection¹⁰¹. They achieved a highly porous coated PHB structure with average pore size of ~ 2 μm . Sandwich ELISA assay was performed to study the detection range of the biosensor. The sensor had 80% specificity and a low limit of detection. It was found that the coated PHB fibers achieved higher sensitivity than the conventional clinical ELISA method¹⁰¹. Hence, it can be expected that the coated PHB electrospun fiber could be integrated into microfluidic or paper-based diagnostic devices with higher performance¹⁰¹.

3. Materials and Methods

The overall purpose of this chapter is to introduce fabrication methods for the production of phage-immobilized PHB substrates and techniques for the characterization of the resulting materials. This will be done to study the efficacy of reporter phage PPO1 immobilized on PHB substrates as a biosensor for the detection of *E. coli* O157:H7. Four types of PHB substrates were prepared (Table 3.1, Fig.3.1), including two types of porous PHB mats (prepared by electrospinning PHB solutions at different concentrations) and two types of PHB films (prepared by solvent casting PHB solutions at different concentrations). The substrates were immobilized with reporter phage PPO1 (expressing the bioluminescent protein Nanoluc) and were used in double agar plaque assay, *E. coli* infection dynamics, *E. coli* capture tests and bioluminescence assay to measure their potential in bacterial sensing of *E. coli* O157:H7. In addition, characterization techniques included water contact angle (WCA) measurements, scanning electron microscopy (SEM), helium ion microscopy (HIM) and fluorescent confocal laser scanning microscopy.

Table 3.1: PHB substrates prepared in this study.

Fabrication method	Process/ Polymer concentration (% w/v)	
	1	5
Electrospinning	Electrospun bead (EB) mat (a)	Electrospun fiber (EF) mat (b)
Solvent casting with plasma treatment	Low concentration solvent-cast (LCSC) film (c)	High concentration solvent-cast (HCSC) film (d)

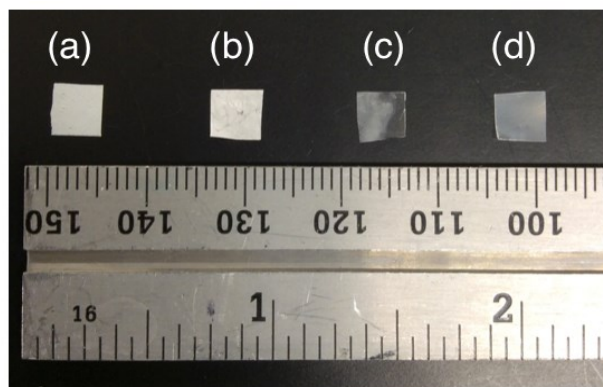


Figure 3.1: PHB substrates prepared in this study. (a).EB mat (1% w/v PHB in chloroform); (b) EF mat (5% w/v PHB in chloroform); (c) LCSC film (1% w/v PHB in chloroform); (d) HCSC film (5% w/v PHB in chloroform).

3.1 Materials

Poly[(R)-3-hydroxybutyric acid] (PHB) of natural origin (No. 29435-48-1, Sigma-Aldrich, St. Louis, MO, USA) was the main material used in this work and was used as received. The molecular weight of the material was approximately 1,070,000 Da with PDI 5.944, according to gel permeation chromatography performed by PolyAnalytik (London, ON, Canada).

Agar (Difco) and Tryptic Soy Broth (TSB, BD B211822, BD™ Tryptic Soy Broth) were purchased from Becton Dickinson and Company, USA. Nano-Glo® Luciferase Assay System (N1110) was purchased from Promega, USA. Phosphate-buffered saline (PBS) was prepared from potassium chloride (KCl), potassium phosphate monobasic (KH₂PO₄), sodium chloride (NaCl), and sodium phosphate dibasic dihydrate (Na₂HPO₄•2 H₂O), following the standard protocol¹⁰² (Table 3.2) These chemicals were purchased from Sigma-Aldrich (Mississauga, Canada).

Table 3.2: Composition of PBS solution

Salt	Concentration (g/L)
KCl	0.2
KH ₂ PO ₄	0.24
NaCl	8.0
Na ₂ HPO ₄ •2 H ₂ O	1.44

3.2 Preparation of Samples

3.2.1 Preparation of PHB Solution in Chloroform

PHB solutions with varied concentrations (1, 3 and 5 % w/v) were prepared by dissolving PHB powder in chloroform. PHB, chloroform and a magnetic stir bar were placed in a 20-ml glass vial with closed lid. The solution was prepared at room temperature and heated on a hotplate at 90 °C with vigorous stirring (500 rpm) for 2 h or until complete dissolution of the polymer. In addition, a thin layer of organic solvent-resistant film was placed in between the lid and opening of the vial to reduce solvent evaporation during heating. Typically, PHB in solutions at low polymer concentration (1 % w/v) dissolved completely within 1 h of heating and stirring. At this point, the polymer solution looked clear and homogenous. The solution was stored in the glass vial at room temperature until further use. Solutions with high polymer concentration (5 % w/v) at room temperature was not as clear as the same solution being heated. On the other hand, solution with low polymer content (1 % w/v) were clear regardless of the processing temperature, as shown in Fig. 3.2.

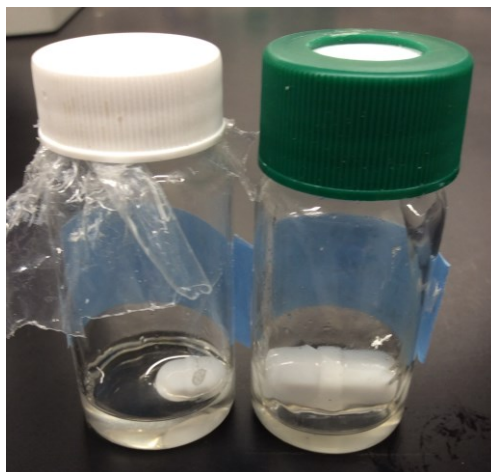


Figure 3.2: PHB solutions at room temperature: 1% w/v (white lid) and 5 % w/v (green lid).

As chloroform is a volatile solvent, it is recommended to prepare a small quantity (10 ml) of fresh polymer solution one day before electrospinning or solvent casting.

3.2.2 Electrospun PHB Substrates

Two different electrospun PHB substrates were prepared and used extensively in this work: one from a solution of 1 % w/v and the other of 5 % w/v PHB in chloroform. Electrospinning the former resulted in beaded fiber mats, whereas the latter produced smooth fiber mats. The schematic and images of electrospinning setup used in this experiment are shown in Figure 3.3, 3.4 and 3.5.

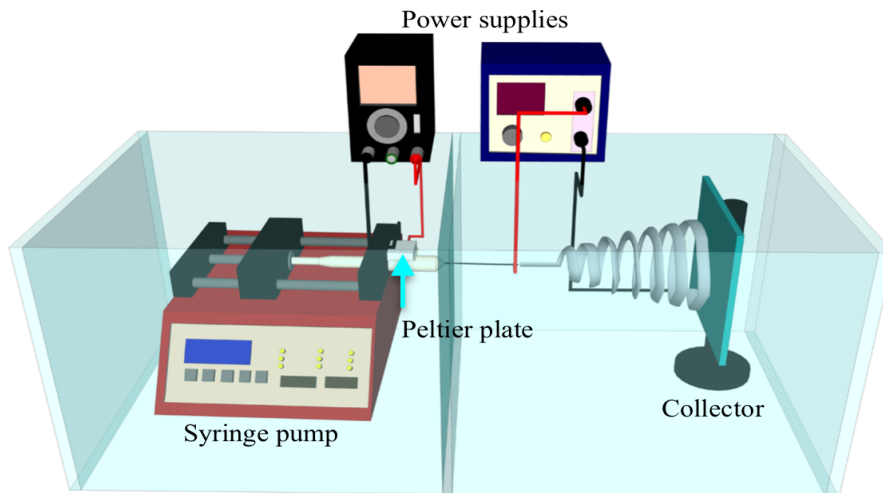


Figure 3.3: Schematic of electrospinning system.

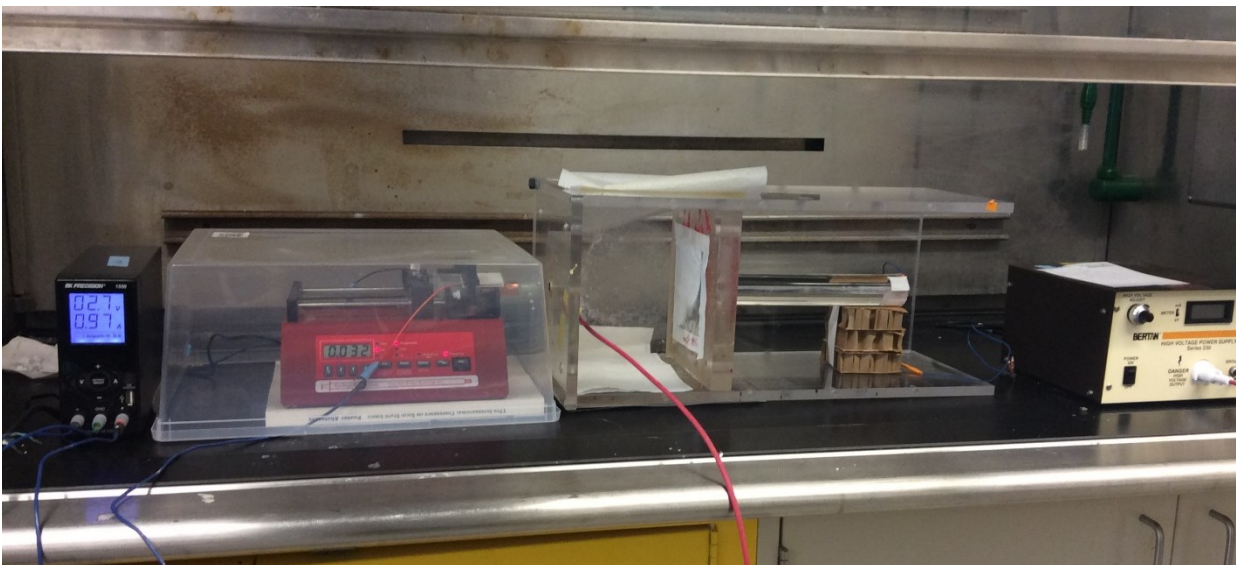


Figure 3.4: Electrospinning setup in chemical hood.

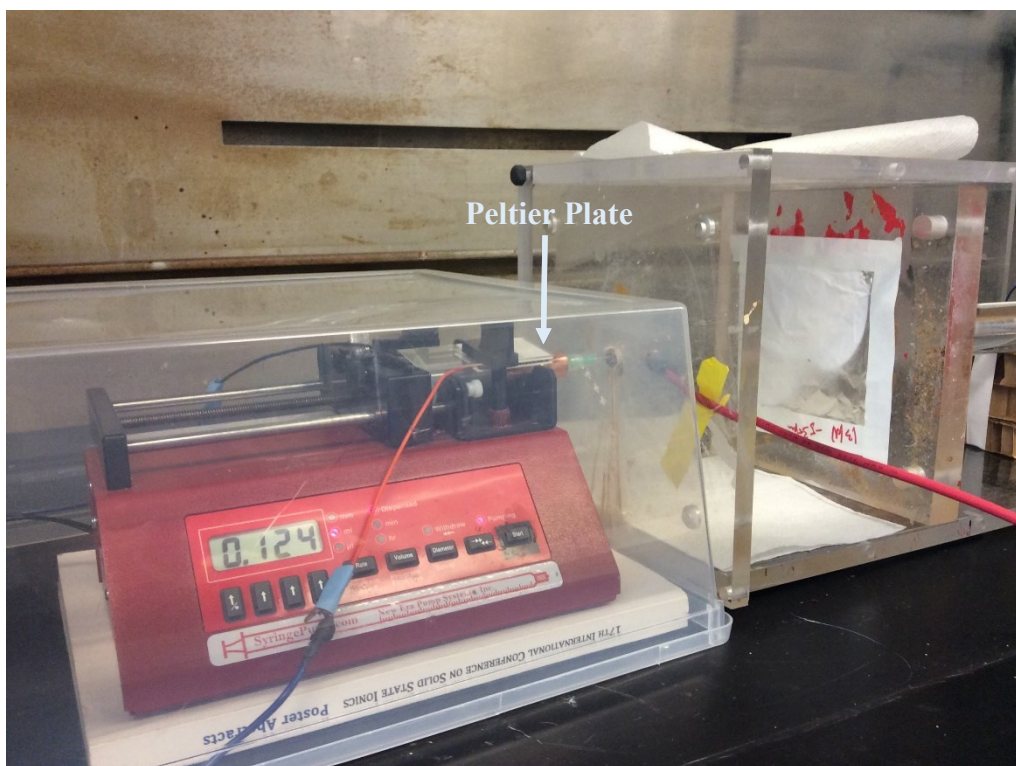


Figure 3.5: Close-up view of electrospinning setup.

The electrospinning system consisted of a syringe loaded with polymer solution, a syringe pump, a copper collector plate, a Peltier plate and two power supplies. The collector plate was covered with a piece of aluminium foil (10 cm \times 10 cm) to aid the collection of the electrospun fibers. The distance between the collector plate and the tip of the syringe was kept at 15 cm at all times. A Peltier plate of 4 cm \times 4 cm (430160-502, HT8 12, Laird Thermal Systems, Morrisville, NC, USA) was placed on top of the syringe to increase the temperature of the polymer solution (Fig. 3.5). This reduced the viscosity of the polymer solution thus facilitating the formation of smooth fibers. The current supplied to the Peltier plate was kept at 1 A, which brought the temperature of the syringe to approximately 50 °C. This temperature was confirmed by a thermocouple fixed at the contact point between the syringe and the Peltier plate. The process of electrospinning was done inside the chemical hood due to high volatility of chloroform. In

addition, the syringe pump, syringe and Peltier plate were placed in an enclosed chamber (36cm × 16.5 cm × 34cm) to avoid heat loss to the environment.

5 ml of PHB solution was fed into a 10-ml syringe fitted with a 21G needle. In order to produce smooth fibers, the ideal pump rate and applied voltage for 5 % w/v PHB solution were set to 0.5 ml/h and 10 kV. Higher flow rates caused dripping of the polymer solution while lower flow rates resulted in polymer clogging the nozzle. Flow rates of 0.1, 0.25, 1 and 3 ml/h were tested. To optimize the applied voltage, 5 kV and 15 kV were also tested. The fiber morphologies that resulted from using these different parameters are shown in the Appendix (Fig. A1).

The 5% w/v polymer solution was electrospun for 6 h under the settings described above to produce smooth fiber mats. However, electrospinning the 1 % w/v polymer solution took much longer time to deposit significant amounts of material on the collector due to its lower polymer content. To increase the efficiency of electrospinning the 1 % w/v polymer solution, the flow rate was adjusted to 5 ml/h. Electrospinning could then be completed within 1 h. The product of electrospinning at this flow rate still produced beaded fiber mats, which were confirmed by scanning electron microscopy (SEM). Both electrospun PHB mats were found to be white and to have a paper-like texture. The size of EB and EF polymer mats were approximately 20 cm² and 64 cm², respectively (Fig. 3.6 and 3.7).

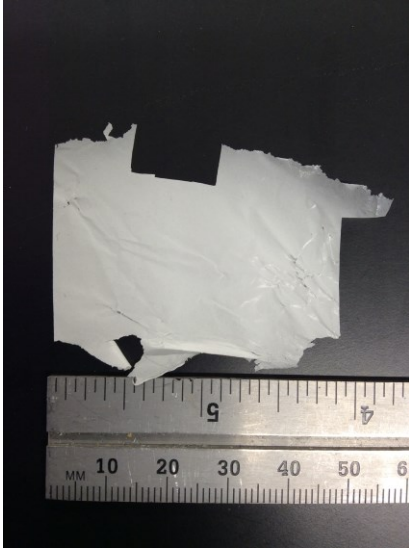


Figure 3.6: EB mat

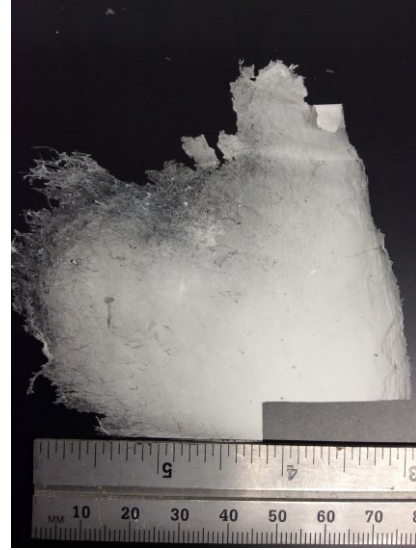


Figure 3.7: EF mat

The fiber mats were trimmed with a pair of scissors to remove the uneven edges. They were then sandwiched in layers of wax paper and cut into squares of 0.5 cm \times 0.5 cm for further experiments.

3.2.3 Solvent-cast Plasma Treated PHB Substrates

Solvent-cast plasma-treated PHB substrates were fabricated using 1 % w/v and 5 % w/v PHB solutions in chloroform. These were used as comparison for the evaluation of phage attachment and *E. coli* infection assays. The PHB substrates were prepared by pouring overnight PHB solution, either 1 or 5 % w/v polymer concentration, on a polyester film layered in a 60 mm (diameter) \times 15mm (height) petri dish at room temperature. The films were then dried overnight in a fume hood. The petri dishes were closed with their lids to avoid rapid evaporation of the solvent, reducing the coffee ring effect¹⁰³ on the casted films.

The resulting films were almost translucent. The thickness of LCSC film was approximately 40 μ m whereas that of HCSC film was approximately 60 μ m. Uneven edges of the films were trimmed off and cut into equal squares of 0.5 cm in length. These films were then treated with

oxygen plasma using Harrick Plasma Cleaner (PDC 001, Harrick Plasma, NY, USA) on both sides of the films, for 1 min each, under high power (30W), at 30 min before experiment.

3.2.4 *E. coli* O157:H7 Cultures

Overnight *Escherichia coli* O157:H7 (ATCC 43888) cultures were prepared by inoculating one colony of *E. coli* O157:H7 from a TSB Agar plate in 10 ml of TSB in a 50-ml shake flask closed with an aerated stopper. The cultures were then incubated overnight in an incubator-shaker (Ecotron, Infors HT, Montreal, Canada) at 37 °C and 250 rpm.

E. coli cultures were initiated by diluting 100-fold of *E. coli* O157:H7 overnight culture with fresh TSB medium in a 50-mL shake flask containing 80% (volume) of headspace. These *E. coli* cultures were incubated at 37 °C and 250 rpm in the incubator-shaker. The growth conditions were recorded by optical density at 600 nm (OD₆₀₀) using a spectrophotometer (Ultrospec 50, Biochrom, UK) hourly. A growth curve was plotted from the data and the log phase was determined to start when the OD₆₀₀ reached 0.2. The time taken for *E. coli* O157:H7 (ATCC 43888) to reach log phase growth was between 45 minutes to 1.5 hours, depending on the volume of *E. coli* culture medium, as well as the environment in the incubator-shaker. These cultures were used to amplify phages or to evaluate the performance of the substrates with immobilized phages.

3.2.5 Phage Amplification

Wild type phage PPO1 were received from Dr. Tanji at the Tokyo Institute of Technology. The reporter phage PPO1 was genetically modified to express the bioluminescent protein Nanoluc by Melissa Harrison at the University of Alberta. The reporter phage stock titer was 2×10⁹ plaque forming units per mL (pfu/ml) and stored at 4 °C in TSB. The bacterium *Escherichia coli* O157:H7 (ATCC 43888) was used as host and target bacterial strain to demonstrate the efficacy of the phage and the materials produced in this study.

Reporter phage stock of PPO1 was prepared through phage amplification in TSB. First, 100 μL of phage suspension at 10^6 pfu/ml were added to 5 ml of fresh log-phase *E. coli* culture. After 15 min at room temperature, the suspension was transferred to 250 ml of TSB medium and incubated in an incubator-shaker (Ecotron, Infors HT, Montreal, Canada) at 37 °C and 250 rpm for 6 h. The phage lysate was collected by filtering the media through a 0.22- μm filter (GSWPO4700, MF-Millipore™ Membrane Filter, MilliporeSigma, Canada). To remove any remaining bacteria cells or debris, the lysate was centrifuged in 50ml round bottom centrifuge tubes (3119-0010, Fisher Scientific, Canada) with an ultracentrifuge (Sorvall RC 6 Plus, Thermo Electron Corporation, Waltham, USA) at $42018 \times \text{rcf}$ for 1.5 h. The supernatant was decanted carefully with a pipette. Then, 1.5 ml of PBS buffer was added to the centrifuge tubes. The phage pellets resuspended in PBS were stored in centrifuge tubes at 4 °C. A phage count was performed the next day to determine the phage titer from the phage amplification, which was approximately 2×10^{10} pfu/mL after centrifugation.

3.2.6 Phage Immobilization on PHB Substrates

Phage immobilization was done by immersing small squares of PHB substrates (0.5 cm \times 0.5 cm) in 2-ml centrifuge tubes containing 100 μL of PPO1 phage suspension (2×10^8 pfu/mL) at 4 °C overnight (Fig. 3.8).

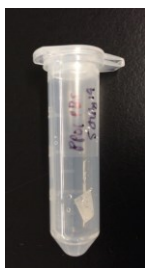


Figure 3.8: Phage immobilization of EF mat in a centrifuge tube containing 100 μL of phage suspension at a titer of 2×10^8 pfu/mL.

3.2.7 Washing of Substrates with Immobilized Phages

On the day of an experiment, prior to their use, PHB substrates were removed from the phage suspension and washed to remove any loosely bound phages. The PHB substrates were transferred to sterile 15-ml test tubes containing 10 ml of PBS buffer. The test tubes were then placed on a rotator (4630 3D Rotator, Lab Line Instruments, IA, USA) for 1 min, allowing the washing liquid to flow freely in the test tubes. Next, the substrates were removed from the test tubes and the buffer was recovered. The substrates were returned to the test tubes, to which 10 ml of sterile PBS buffer were added for a second washing step using the same procedure. In total, four consecutive washing steps were performed using the same procedure, creating a total of 40 ml of wash liquid (spent PBS buffer) for each PHB substrate. Fewer than 10^3 pfu/mL (for a total of less than 4×10^4 pfu released) of non-immobilized phages were detected after the final wash.

3.3 Characterization

3.3.1 Scanning Electron Microscopy

A Zeiss Sigma Field Emission Scanning Electron Microscope (FESEM; Carl Zeiss AG, Germany) was used to study the surface features of the PHB samples as well as the diameter of the electrospun fibers. PHB substrates of 0.5 cm \times 0.5 cm were mounted on circular conductive carbon adhesive tapes on aluminum sample holders. Prior to scanning electron microscopy (SEM), all PHB substrates were coated with a thin film of carbon (10 nm in thickness) with a Leica ACE 600 coater (Leica Microsystems GmbH, Germany) to avoid surface charges on the samples during imaging. The electron high-tension voltage was 3 kV, which allowed obtaining clear images without destroying the delicate samples.

3.3.2 Water Contact Angle Measurement

Contact angle measurements were performed to determine the hydrophilicity and surface roughness of samples. For each experimental condition, three samples of 0.5 cm × 0.5 cm PHB substrates were prepared. The samples were fixed on glass slides with double-sided tape (Fig. 3.9).

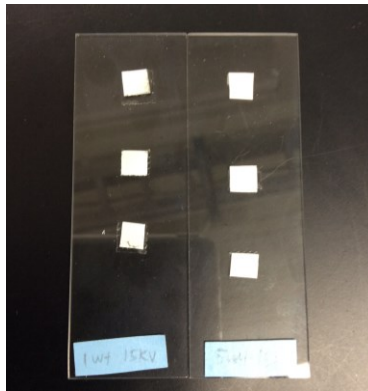


Figure 3.9: Electrospun samples prepared for WCA measurements. Triplicate are shown for two different conditions tested.

The tests were done using the sessile drop method on a Video Contact Angle 2000 System (AST Products Inc., Billerica, MA, USA) with deionized water. The measurements were recorded 30 sec after the water drop contacted the surface.

3.3.3 Double Agar Phage Plaque Assay

The double agar plaque assay was used to determine phage titer. First, 20 ml of hot 3 % w/v agar TSB solution was poured on petri dishes (60 mm in diameter × 15 mm in height). Next, 100 μ l of phage suspension and overnight *E. coli* culture were mixed with a warm (45 °C) 1.5 % w/v agar TSB solution. The mixture was added on top of the hardened agar in the petri dishes. Once the newly added agar solidified, the plates were incubated at 37 °C overnight to allow for the apparition of plaques resulting from phage infection. A phage count was performed the next day

by enumerating total plaques (plaque forming units; PFU) on the agar plates and converting to a phage titer (PFU/ml) when required.

3.3.4 Phage Loading on PHB Substrates

In order to determine the phage loading on each substrate produced, phage loading tests were performed. In these, the phage titer of the phage suspension used for immobilization, along with its volume, were determined before and after immobilization. First, the mass of each PHB substrate and two glass slides of 75 mm × 25 mm were measured and recorded. Then, phages were immobilized on the substrate overnight with 100 µl of phage suspension at 10⁹ PFU/ml at 4°C. After overnight immobilization, substrates were removed with a pair of forceps and sandwiched between two glass slides to measure the mass of the phage-immobilized substrate. 50 µl of the remaining lysate was serially diluted with PBS buffer and used in the double agar plaque assay to determine the phage titer of the remaining lysate after immobilization. The difference in phage titer was used to assess the amount of phages loaded on the substrate.

3.3.5 Phages Release After Washing

The number of phages released from substrates after washing were enumerated using the double agar plaque assay. 1 ml of wash liquid (spent PBS buffer) was collected from each wash as described in section 3.2.8. After the wash, 100 µl of the collected wash liquid was serially diluted with PBS buffer and then plated to determine the phage titer. This was converted to a number of phages released from the substrate during washing.

3.3.6 Fluorescent Confocal Laser Scanning Microscopy

The fluorescent confocal microscopy was performed on phage-immobilized PHB fiber mats (electrospun fiber, 0.5 cm × 0.5 cm) using a Zeiss Axio Imager M2m (Carl Zeiss AG, Germany) to study the distribution of phages after immobilization on the substrate. A fiber mat without

phages was used as the control. Both fiber mats were dehydrated with dilutions of ethanol (1 ml at 25%, 50%, 80%, and 100%) and fixed with 100 μ l of glutaraldehyde solution. After that, 10 μ l of diluted solution of SYBR green I stain (Life Technologies, Carlsbad, USA) were dropped on top of each mat. The mats were shielded from light for 30 min before rinsing with 1 ml of PBS buffer to remove excess dye. Next, the mats were placed on a glass slide. A drop of antifading agent (SlowFade Gold Antipode Mountant, Thermo Fisher Scientific Inc., MA, USA) was added before placing the cover slide. The imaging was performed using a 258 nm filter with a mercury lamp as light source. Images were taken at the edge and center of the substrate sample to investigate edge effects on immobilization.

3.3.7 Helium Ion Microscopy

Helium Ion Microscopy (HIM) was used to study the attachment of immobilized phages on individual fibers of electrospun substrates. 0.5 cm \times 0.5 cm of PHB substrates were immobilized with phages and used in this microscopy. PHB substrates without immobilized phages were used as control. Both samples were mounted on circular studs with conductive carbon adhesive tapes, similar to the preparation of SEM samples (Fig. 3.10). All substrates were dehydrated and fixed following the protocol described in Section 3.3.6 prior to microscopy.

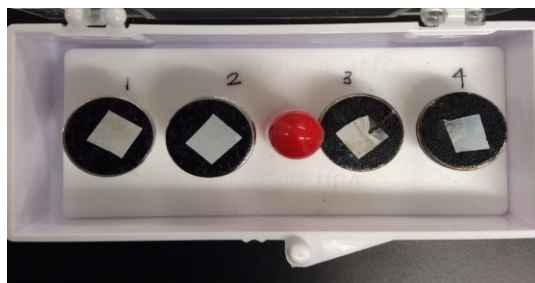


Figure 3.10: Phage-immobilized PHB substrates mounted on studs for Helium Ion Microscopy.

3.3.8 Phage Infection Dynamics

The purpose of this experiment was to show the infectivity of phage PPO1 after immobilization, as well as, to compare performances of different phage-immobilized PHB substrates. All four types of PHB substrates were immobilized with 100 μ l of phage suspension and washed, as described in the previous sections. On the day of an experiment, 10 ml of fresh *E. coli* culture were prepared and incubated at 37 °C and 250 rpm in an incubator shaker until the OD₆₀₀ of the cell culture reached 0.2 (corresponds to 10⁸CFU/ml of cell culture). Then, a phage-immobilized film (0.5 cm \times 0.5 cm) was immersed in the *E. coli* suspension and incubated at the same conditions (Fig. 3.11). OD₆₀₀ measurements were taken with a spectrophotometer every hour for 5 h. Triplicates were performed for each experimental condition. Pure *E. coli* cultures were used as control.

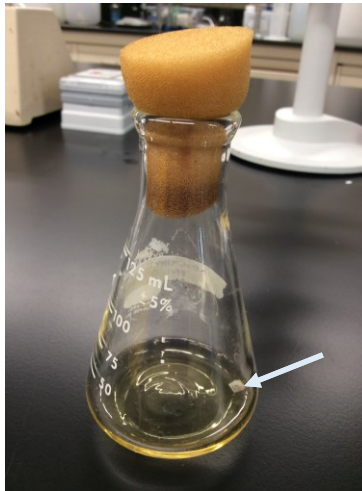


Figure 3.11: A phage immobilized EF mat (indicated by arrow) immersed in *E. coli* suspension.

3.3.9 Bioluminescence Assay

To perform the bioluminescence assay, 15 μ l of NanoGlo luciferase substrate (N1110, Promega, Wisconsin, USA) was mixed with an equal volume of phage sample and placed on an opaque white 96 well plate (CLS 3362, Corning Inc., New York, USA). A luminescent plate

reader (Biotek, Winooski, VT, USA) was used to measure the bioluminescence of the samples, reported as relative luminescence units (RLU).

3.3.10 *E. coli* Capture Test

An *E. coli* capture test was used to probe the question of which PHB substrate was able to capture more *E. coli* cells, which is expected to correlate with the infectivity of phage-immobilized substrates. First, the phage-immobilized PHB substrates were immersed in 1 ml of log phase *E. coli* culture at an OD₆₀₀ of 0.2 for 1 min, then transferred to 6 ml of sterile TSB in 50-ml conical flasks. The flasks were incubated at 37°C and 250 rpm for 3 h. 1-ml samples were taken out for bioluminescence measurement every hour. Phage-immobilized films of each type of PHB substrate without contact with *E. coli* were used as controls.

3.3.11 Bioluminescence Assay of EF Mat

A bioluminescence assay was performed for EF mats exposed to *E. coli* to determine the limit of detection of the biosensor. 0.5 cm × 0.5 cm of phage-immobilized EF mats were incubated with 10 ml of log phase *E. coli* dilutions at 10², 10⁴, 10⁶ and 10⁸ CFU/ml in 50-ml conical flasks. The flasks were incubated at 37°C and 250 rpm. 1-ml samples were taken from the flasks for bioluminescence measurements every hour for 4 h.

3.3.12 Swab test of EF Mat

A swab test was carried out to investigate the application of phage-immobilized PHB fiber mats for detection of *E. coli* O157:H7 in TSB medium and milk. First, the EF PHB samples were cut into squares (0.5 cm × 0.5 cm), immobilized and washed as described in previous sections. The samples were immersed in 1 ml dilutions of *E. coli* at 10¹, 10³, 10⁵ and 10⁷ CFU/ml and placed on a rotator (4630 3D Rotator, Lab Line Instruments, IA, USA). After 1 min contact time with *E. coli*, the bacteria loaded samples were transferred to 1 ml sterile TSB contained in a 24-well plate and incubated for 4 h at 37°C and 250 rpm (Fig. 3.12). 50-μl samples were taken out

for bioluminescence measurement every hour. Phage-immobilized mats with no contact with *E. coli* were used as controls. The experiment was done in triplicates.



Figure 3.12: A 24-well plate containing phage immobilized PHB substrates and TSB media.

4. Results and Discussion

This chapter focuses on presenting and discussing the results obtained in this study. It begins with the characterization of both porous electrospun PHB mats and flat PHB films by scanning electron microscope and water contact angle measurement. Then, phage attachment to different PHB substrates was examined through helium ion microscopy and fluorescent confocal laser scanning microscopy. In addition, the phage loading on and phage release from various PHB substrates were evaluated, followed by the analysis of *E. coli* infection dynamic assays and *E. coli* capture tests. Finally, a bioluminescence assay was conducted with the most promising material samples to validate the bacterial sensing property of the phage-immobilized PHB substrates in detecting *E. coli* O157:H7.

4.1 PHB Sample Characterization

In this work, solutions composed of 1 % w/v or 5 % w/v PHB in chloroform were processed through electrospinning and solvent casting to produce four entirely different substrates. Electrospun mats produced from 1 % w/v PHB solution with beaded morphology are referred to as ‘electrospun bead (EB) mats’, and electrospun mats produced from 5 % w/v PHB solution with fibrous morphology are referred to as ‘electrospun fiber (EF) mats’, films made from 1 % w/v PHB solution are referred to as ‘low concentration solvent-cast (LCSC) films’ and films made from 5 % w/v PHB solution are referred to as ‘high concentration solvent-cast (HCSC) films’. The characteristics of the samples used for experiments are summarized in Table 4.1.

Table 4.1: Mass and thickness of each PHB substrate used in the study. All samples were squares of equal area (0.25 cm²).

PHB substrate	Mass (mg)	Thickness (μm)
EB mat	0.52 ± 0.06	43 ± 6
EF mat	0.32 ± 0.02	40 ± 0
LSCS film	0.42 ± 0.02	13 ± 6
HSCS film	2.65 ± 0.08	80 ± 10

The mass and thickness of the samples were different for each type of PHB substrate, ranging from 0.32 to 2.65 mg and from 13 to 80 μm , respectively. HSCS films had the highest mass and were also the thickest. The lightest samples were obtained from EB mats. The thinnest samples were LSCS films.

The surface morphology of the above-mentioned PHB samples was studied by scanning electron microscopy (SEM; Fig. 4.1).

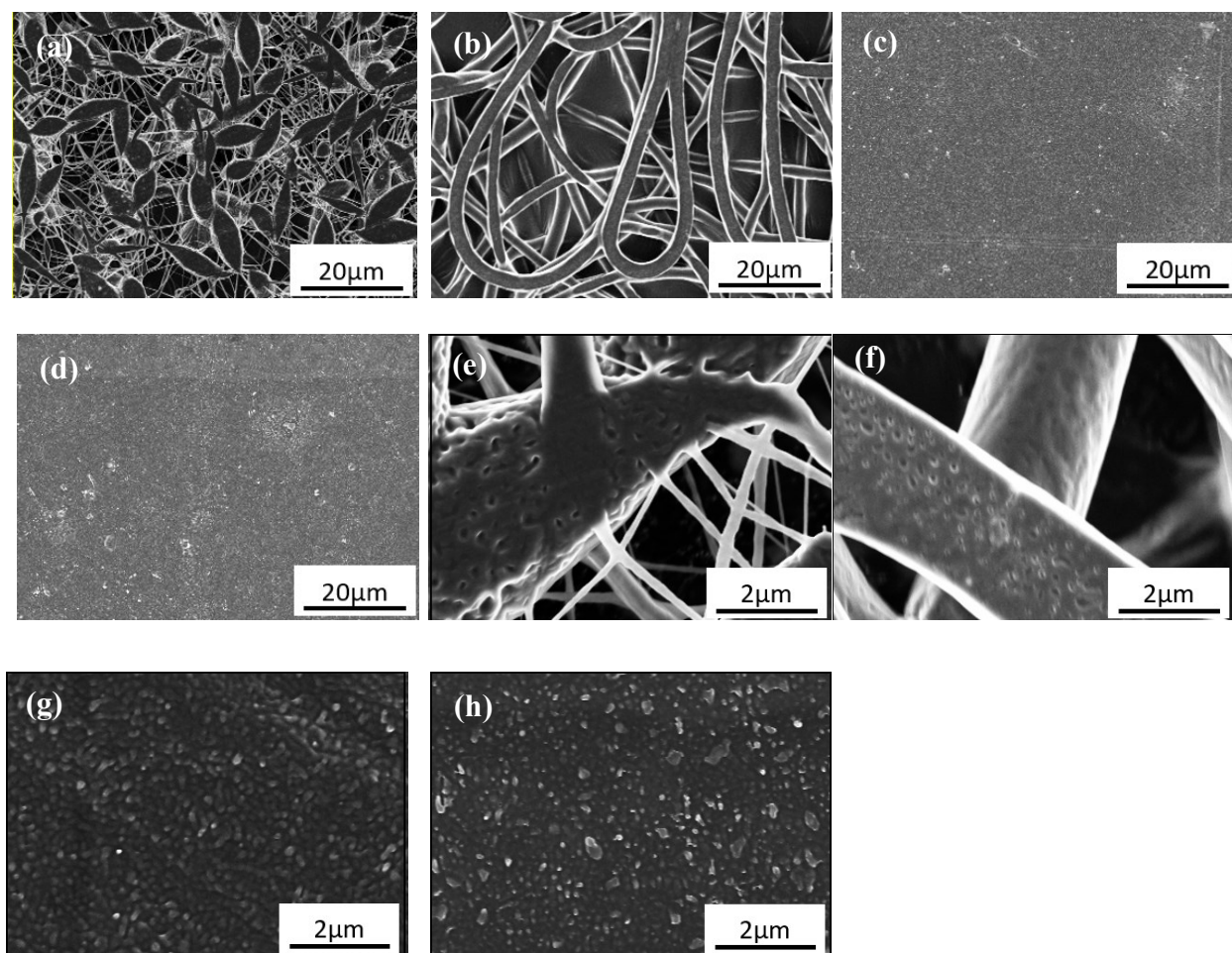


Figure 4.1: Scanning electron microscopy of a,e) EB mats, b,f) EF mats, c,g)LSCS film and d,h) HSCS film.

Electrospinning of 1 % w/v PHB in chloroform formed non-homogenous fibers ($0.48 \pm 0.2 \mu\text{m}$) with spindle-like beads ($3.75 \pm 0.7 \mu\text{m}$) of various sizes separated by fine filaments ($0.15 \pm 0.03 \mu\text{m}$) (Fig. 4.1 a, EB mats). The images at higher magnification revealed that the surface of

beads was rough (Fig. 4.1 e). On the other hand, electrospinning of 5 % w/v PHB produced smooth fibers with a consistent diameter of $2.78 \pm 0.5 \mu\text{m}$ (Fig. 4.1 b, EF mats). The fibers were randomly aligned with voids found between them. Qualitatively, the void space was greater for the EF mats than for the EB mats. Similar to the surface of the EB mats, high magnification of SEM images showed the surface of EF mats had many indentations (Fig. 4.1 f). In contrast, both plasma treated films produced from solvent casting (Fig. 4.1 c, d) were smooth and flat. However, under higher magnification, nodules were seen from both films (Fig. 4.1 g, h). Larger, irregular nodules were found on the HSCS film than the LCSC film.

The thickness of electrospun PHB samples differed, which can be attributed to the fact the collection time for the different sample types differed due to the difference in solution concentration. The time point to collect the mats was judged by mere observation, and corresponded to a time when the electrospun mats were thick enough to be peeled off from the collector plate. Therefore, the thickness of the PHB samples was not tightly controlled. For the solvent-casted films, the HSCS film was significantly thicker than the LCSC film, due to higher amount of polymer in the casting solution.

It is well known that, in electrospinning, polymer concentrations greater than the critical entanglement concentration are required to achieve smooth fiber production⁸⁸. The critical entanglement polymer concentration of PHB ranges from 5 to 14 % w/v, depending on the molecular weight of the polymer^{94,104,105}. 5 % w/v PHB solution was determined to be above the critical entanglement polymer concentration, where homogeneous fiber mat was obtained from electrospinning, as seen from the SEM images (Fig. 4.1 b). At the lower concentration of polymer in solvent (1 % w/v), which is below the entanglement concentration, electrospinning formed drops rather than continuous fibers as the repulsive charges dominated the system, breaking the polymer jet into fragments of droplets, resulting in the formation of beads as observed in Fig. 4.1 a, e. The formation of such beads is indicative of insufficient chain

entanglements. The transition from non-uniform beaded fiber to homogenous fiber can be observed by electrospinning 3 % w/v PHB solution (Appendix A.1).

The SEM images at higher magnification show the surface of electrospun beads and fibers were rough and presented indentations, which typically result from rapid phase separation during the electrospinning process as the solvent rapidly evaporates. During the evaporation, the polymer-rich phase forms a part of the fiber matrix while the solvent-rich phase results in the formation of surface indentations⁹⁴. This phenomenon was also found on electrospun polystyrene fibers⁹⁴.

On the other hand, nodules were observed from both solvent-cast films. It is postulated that these nodules were the crystallized domains of PHB due to slow evaporation process¹⁰⁶.

4.2 Wettability

The wettability of PHB substrates is one of the factors affecting phage immobilisation^{54,107,108}. In order to obtain water contact angle (WCA) values, the sessile drop method was performed on 3 samples of each type of PHB substrate produced in this study. The WCA measurements and representative images are shown in Fig. 4.2.

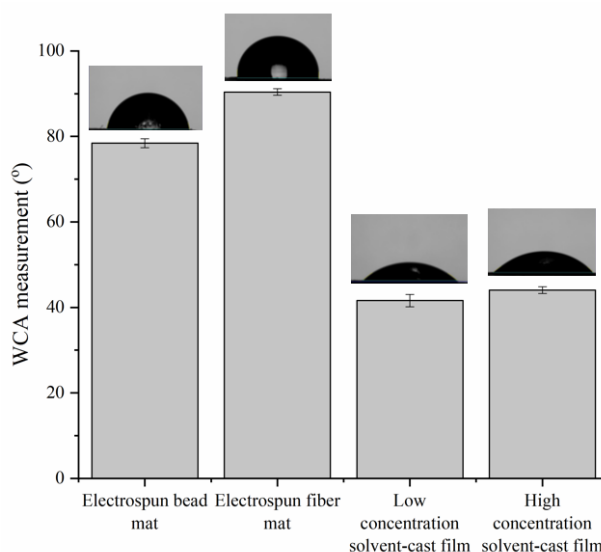


Figure 4.2: Water contact angle (WCA) measurements of PHB substrates.

Based on Fig. 4.2, there is a clear distinction in WCA values between the electrospun mats and plasma treated thin films. The electrospun PHB mats had higher WCA, and thus were more hydrophobic, than the cast thin films. The average WCA values of electrospun mats were 79.43° and 90.40°, for EB and EF mats, respectively. On the other hand, the plasma treated PHB films had WCA values around 41.59° and 44.03° for LCSC and HCSC, respectively. The static WCA value of a hydrophobic surface is 65° or greater, while a hydrophilic surface has a WCA below this value¹⁰⁹. Therefore, both electrospun mats were considered hydrophobic while the thin films were hydrophilic.

It was hypothesised that electrospun PHB mats would exhibit higher WCA due to their rougher surface, as explained by Cassie's law¹¹⁰. According to the theory, air gaps occur between solid surface areas in a porous medium, minimizing the contact area between water and the solid. Therefore, as more air is trapped in a material with a rougher surface, the contact angle greatly increases. Plasma treatment changes the surface wettability of PHB films from hydrophobic to hydrophilic due to changes of chemical composition of the surface. Functional groups such as carboxyl, hydroxyl, and peroxide groups have been shown to form on the polymer surface through incorporation of oxygen after plasma treatment⁵⁴. The addition of polar components onto the surface significantly increases the surface energy^{54,111}.

PHB has been demonstrated to be a relatively hydrophobic polymer. Some of the reported WCA values for pristine PHB surfaces range from 68° to 96.83°^{94,54,111}. As for electrospun PHB fiber mats, reported values in the literature were 115.5° and 117°^{94,101}. The disparity between the reported WCA values could be due to the types of solvent used in the tests. Solvents of different volatility have different evaporation rates, thereby influencing the surface roughness of the polymer products, whether the production process is solvent casting or electrospinning.

4.3 Phage Loading

Phage loading on the PHB substrates per surface after overnight exposure was calculated to estimate the upper limit of the density of immobilized phages. It was calculated from measurements of the titer and volume of phage lysates before and after immobilization, using the following formula.

$$\text{Number of phages loaded per surface} = \frac{C_i V_i - C_f V_f}{A}$$

where C_i represents initial phage titer of the lysate before immobilization, V_i for initial volume of phage lysate, C_f represents final titer of the lysate after immobilization, V_f for final volume of remaining phage lysate and A for surface area of PHB substrates.

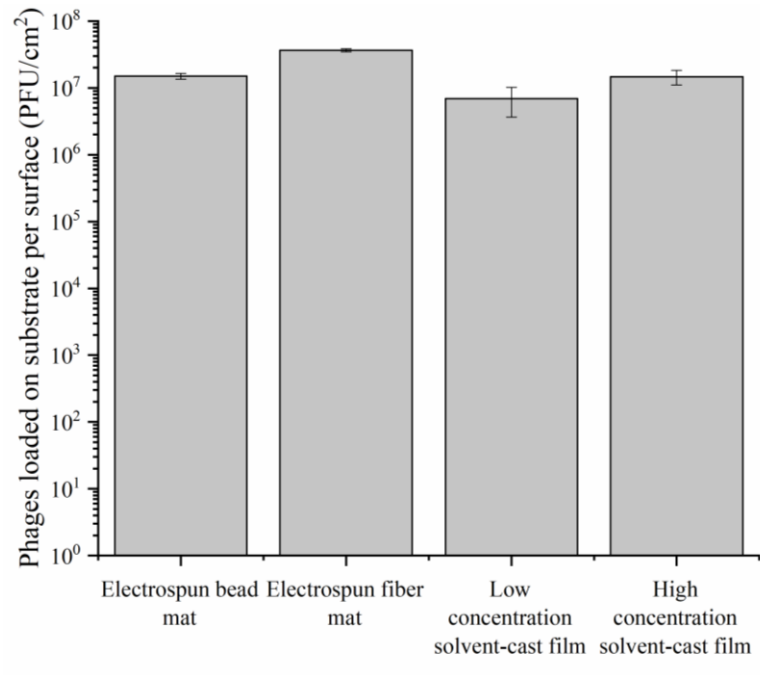


Figure 4.3: Number of phages loaded on substrates per surface, assuming no volume loss of phage lysate during overnight immobilization. Triplicates were performed for these experiments.

The number of phages loaded on the substrates per surface were 1.50×10^7 PFU/cm² on EB mat, 3.66×10^7 PFU/cm² on EF mat, 6.92×10^6 PFU/cm² on LCSC film and 1.47×10^7 PFU/cm²

on HCSC film. EF mat had most phages on the substrates, followed by EB mat, HCSC film and LCSC film. However, the p-value of the data set (based on a two-way ANOVA test) was found to be 0.965, meaning the values of phage loading on each PHB substrate were not significantly different, which is likely caused by experimental error and the scale and sensitivity of the titer measurements.

4.4 Phage Release after Immobilization

To quantify the number of phages released from PHB substrates after immobilization, the phage-immobilized substrates were washed four times with 10 ml of PBS buffer. The buffer was collected and the number of phages released was enumerated using the double agar plate assay.

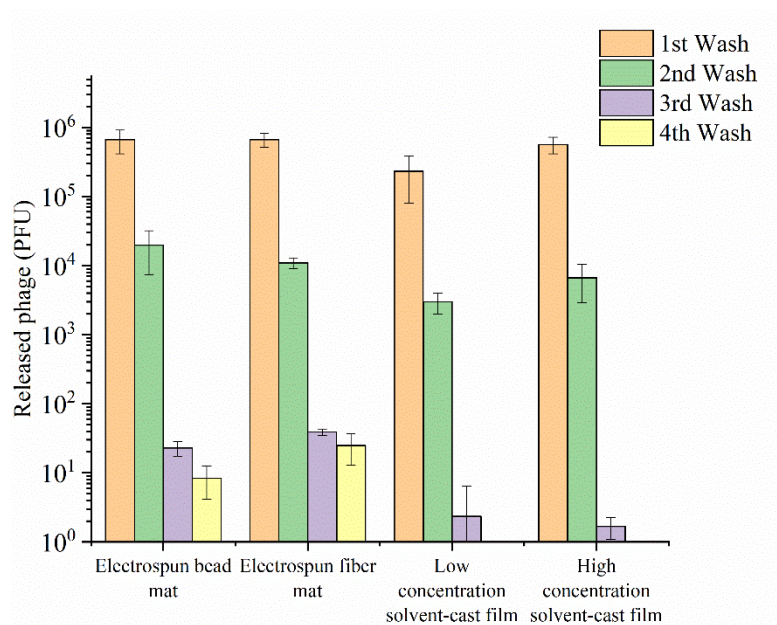


Figure 4.4: Phages released from PHB substrates during washing. Average values and standard deviations are reported and were based on triplicate measurements.

For each substrate more phages were released with the first wash – ranging from 2.33×10^5 PFU for the LCSC film to 6.67×10^5 PFU for the EF mats. The number of phages released gradually reduced with each washing step. The plasma treated films did not release any phages after the third wash, whereas the electrospun mats continued to shed phages with additional washing. At the fourth wash, the EB and EF mats still released approximately 8.33 PFU and 24.7

PFU, respectively. P-value obtained from two-way ANOVA test was 0.002, which showed that the group of data was significantly different.

The number of phages released after immobilization could affect the infectivity of phage-immobilized substrates. It is postulated that some of the phages present in the electrospun membranes were held by mechanical retention in the mesh network, in addition to adsorption on the fibers and beads. During the washing steps, phages that are retained in the outer layer of the electrospun membranes (but not adsorbed) may be released. However, phages that are deeper within the interstitial spaces of the network may be trapped and not in contact with the washing fluid due to the hydrophobic nature of PHB. Therefore, at least some of the phages could remain in electrospun membranes (even after several washes) and could then be, slowly released to the surroundings. On the other hand, phages attached on the plasma treated flat films were presumably bounded by electrostatic attraction between the hydroxyl group and phage capsid. In this case, unbound phages are thus expected to be washed away from the surface of the PHB films, leaving only strongly attached phages, which would explain why no phages were released by the third washing step. Through these tests, it can be hypothesized that phages were not as readily released from the electrospun membranes as from the plasma treated flat films.

4.5 Phage Attachment on PHB Substrates

A closer look at the attachment of phage PPO1 to PHB substrates was obtained via helium ion microscope (HIM). The distribution of phages on the material are shown in Fig. 4.5. Control samples without phages were included for reference.

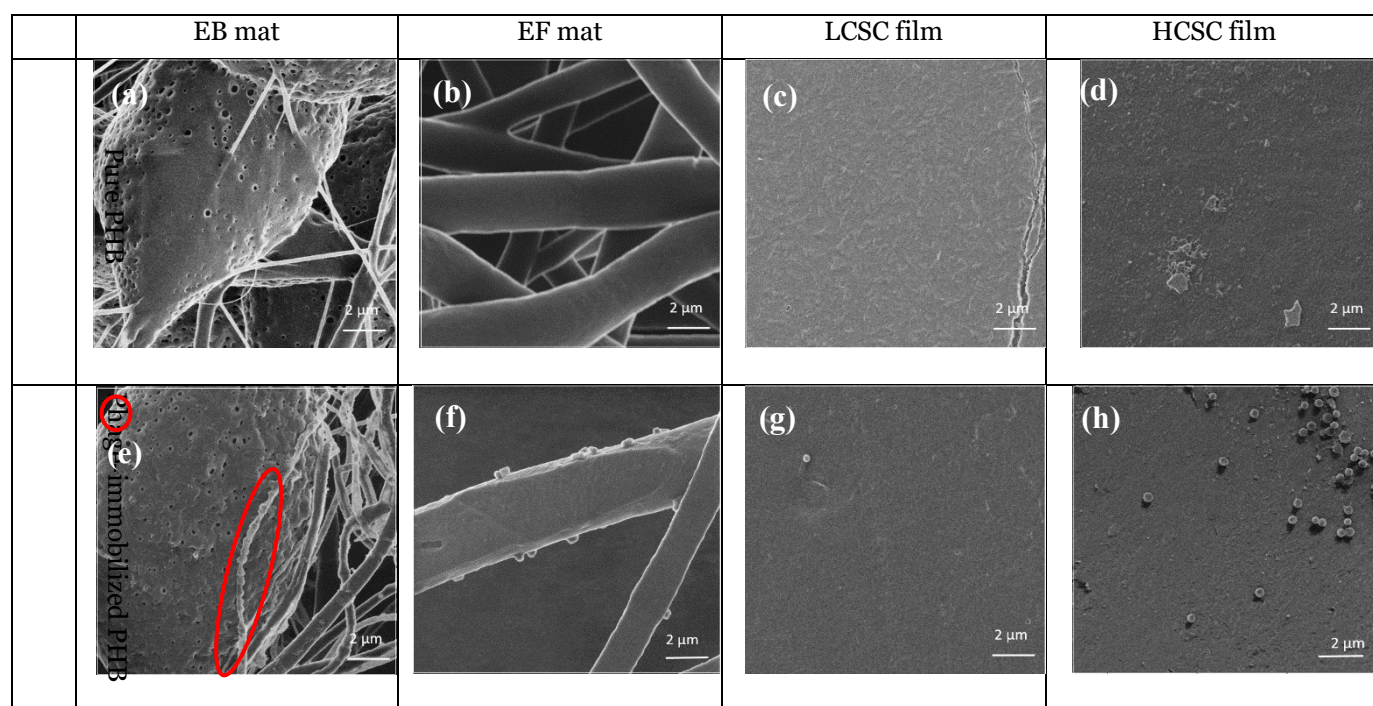


Figure 4.5: Imaging of phage particles immobilized on PHB substrates (EB mat, EF mat, LCSC film and HCSC film) using helium ion microscopy. Images are shown for each substrate, and for each substrate exposed to phages (phage-immobilized after 4 washing steps). Images were taken at 4 different locations of PHB substrates. The images collected with the most number of phages were presented.

Phages were observed on all PHB substrates. On EB mats (Fig. 4.5 e), phages were found on both fibers and beads. Interestingly, there were more phages visible on the fibers than the beads. For the phage-immobilized EF mat (Fig. 4.5 f), phages were observed on the fibers with no preferred orientation. Only a single phage particle was found on LCSC film (Fig. 4.5 g) while more phages were seen on HCSC film (Fig. 4.5 h). These images were not considered to be quantitative as only small areas of sample were captured, but they can serve as a qualitative assessment of the phage immobilization on the materials.

The attachment of phage PPO1, as shown in these HIM images (Fig. 4.5), was distributed across the surfaces. Clustering of phages could be observed (Fig. 4.5 e, f, h), which is in line with previous results as reported by Naidoo et al., who studied surface attachment isotherm of T4 bacteriophage on planar surface⁵⁹. Unexpectedly, surface attachment of phages did not occur

according to the idealized Langmuir isotherm, which assumes all adsorption sites have equal sorption energies, resulting in homogenous surface attachment of phages. In fact, the microscopy images suggest that the surfaces were highly heterogeneous. One possible explanation was that initial attachment of phages could lower the surface energy for additional phage attachment, thereby facilitating surface aggregation of phages⁵⁹.

4.6 Phage Distribution on PHB Substrates

The distribution of phages on the surface of a material is critical in assessing its performance and understanding the mechanisms leading to phage immobilization and interactions with host cells.

In this study, phages were immobilized on EF mat, then stained with SYBR green I and visualized through fluorescence confocal laser scanning micrographs. Fig. 4.6 shows the distribution of phages on the center (Fig. 4.6 a, b) and edge (Fig. 4.6 c, d) of the substrate. Under the imaging conditions, stained phages appeared in green while the PHB polymer appeared in blue (due to autofluorescence).

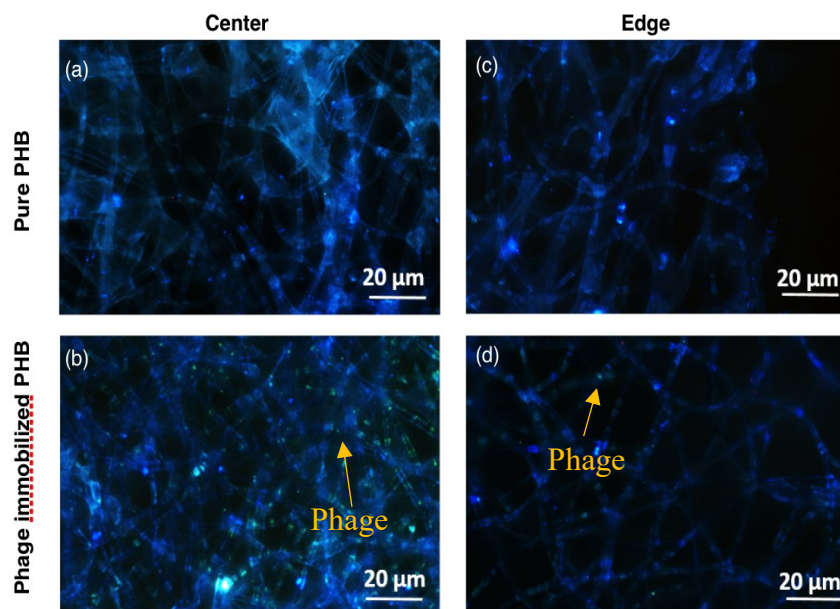


Figure 4.6: Fluorescent confocal microscopy images of PHB electrospun mats incubated with phage suspensions containing 10^9 PFU/ml. Imaging was made at the center (a, b) and edge (c, d) of the PHB control mats (a, c) and the PHB mats with phages (b, d). Phages, stained with SYBR green I, appear in green; PHB fibers appear in blue due to autofluorescence.

As can be seen, more phages were located at the center, rather than at the edge, of the film (Fig. 4.6 b, d). This phenomenon may be due to detachment of phages from the edge of fibrous mats during washing step prior to staining or during handling. It is very probable that phages that penetrated the films more deeply were not captured by the confocal imaging. Unfortunately, the depth of the image was limited due to interferences from the overlapping fiber network.

4.7 Phage Activity on PHB Substrates

The comparison of the *E. coli* infection dynamics in the presence of the different substrates with immobilized phages provides information on both the ability of the substrates to immobilize phages and the activity of these immobilized phages. PPO1 phages were immobilized on PHB substrates of equal dimensions (0.25 cm^2) by exposing the latter to $100 \mu\text{l}$ of 10^9 PFU/ml phage suspension. The substrates were then washed with 10ml of PBS for four times, to

remove unbound phages and placed in cultures of *E. coli* O157: H7 to measure infectivity of the phages immobilized on PHB substrates.

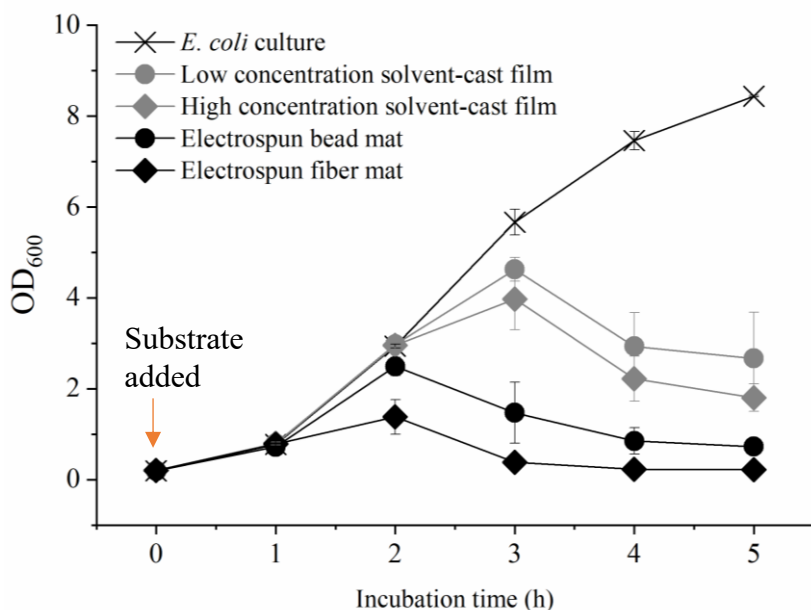


Figure 4.7: Phage-immobilized PHB substrates (0.25 cm²) were incubated with *E. coli* O157: H7 for 5 h. The results are presented with standard deviations from triplicates. Arrow indicates the time point where substrates were added to the culture.

In these experiments, cultures of *E. coli* in the absence of phages were monitored as control. Figure 4.7 shows that the optical density of the uninfected *E. coli* steadily increased over time, indicating growth of bacteria during the incubation period. The phage-immobilized substrates were immersed in the cultures when these entered exponential growth to maximise phage replication. The optical density (OD₆₀₀) of all cultures exposed to phage-immobilized substrates briefly increased then gradually decreased as the infection proceeded and cells lysed. Exposure to the phage-immobilized EF mat resulted in complete lysis of the *E. coli* populations within 3 h. The other materials, in order of shortest to longest time to reach complete lysis were the EB mat, HCSC film and LCSC film. A two-way ANOVA test was performed to measure the statistical significance of the result. The difference between each substrates was found to be significant (p-value<0.05).

As anticipated, phage-loaded EF mat demonstrated higher infectivity than the EB mat. The infectivity of both phage-immobilized electrospun mats was also greater than that of solvent-cast films (Fig. 4.7).

4.8 *E. coli* Detection in Cultures

To study the interaction between bacteria and immobilized phages, the *E. coli* capture efficiency tests were performed by first immersing PHB substrates with immobilized PPO1 phages modified to express the bioluminescent protein Nanoluc into a suspension of *E. coli* cells in the exponential phase. After 1 min of exposure to the culture, the substrates were then transferred and incubated in sterile TSB medium for 3 h, and the bioluminescence of the liquid medium was measured hourly.

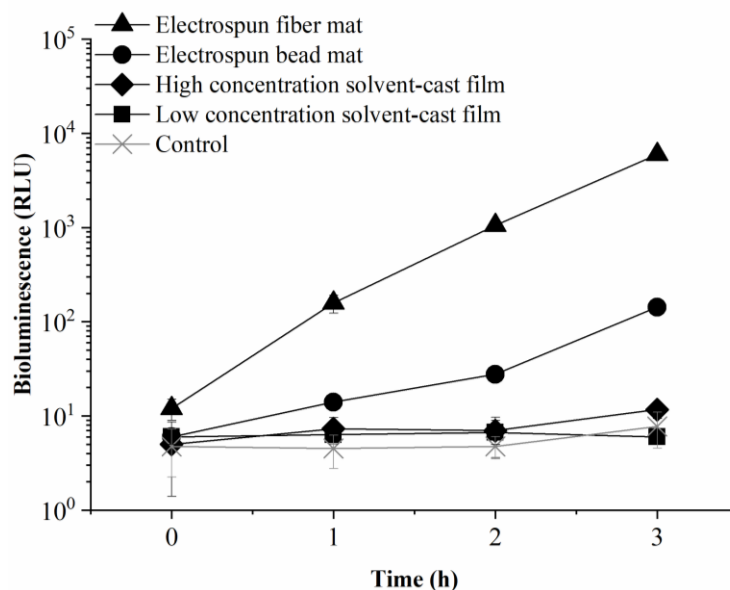


Figure 4.8: Detection of the presence of *E. coli* cells in a culture by PHB substrates with immobilized phage PPO1 modified to express Nanoluc, as measured by bioluminescence. Triplicate measurements were performed, and average values and standard deviations are shown (in some cases the size of the error bars is smaller than the data points). Control condition is the average measurement of 4 samples consisting of only PHB substrate (no phage), one for each type of PHB substrate.

In these experiments, Nluc proteins released upon infection of *E. coli* O157:H7 cells by the modified PPO1 phage are reacted using the Nluc assay to produce the bioluminescent signal. The

Nluc gene is injected into the host when a reporter phage PPO1 infects the host cells. As phages replicate within the bacterium, Nluc proteins are produced. Therefore, substrates containing the most bacteria will be able to produce the most Nluc proteins, thereby creating the strongest bioluminescence signal.

As can be seen in Figure 4.8, the strongest bioluminescence was observed for the EF mat, which was apparent from the early stages of the experiment and which led to a signal 3-orders of magnitude greater than the control after 3h. The EB mat came second, with a signal 1-order of magnitude stronger than the control after 3h. The bioluminescence signals obtained from plasma-treated films were very weak, being on the same order as that of control samples. The HCSC film showed a small increment in bioluminescence after 3 h, while the signal from the LCSC film remained fairly constant throughout the experiment. A p-value < 0.05 was found by two-way ANOVA test, meaning the experimental result was significantly different from each group of sample.

From these results, it can be seen that more bacteria were captured and infected by the electrospun PHB mats with immobilized phage than the solvent-cast films with immobilized phages, contributing to a higher bioluminescence signal. The porous fibrous structure of electrospun fibers is interconnected, promoting bacteria cell adhesion thus increasing the frequency of phage-host cell binding. On the other hand, since the plasma-treated films were flatter, their morphology and limited surface area decrease the likelihood of frequent phage-host encounters. Also, as *E. coli* cells are charged and thus have electrostatic repulsion between each other, close packing of bacteria on the surface of the plasma-treated films was unlikely⁵⁷.

4.9 Performance of Phage-based Material for *E. coli* O157:H7 Detection

Initially, small squares of EF mats on which Nanoluc reporter phage PPO1 were immobilized were used as biosensors to detect *E. coli* O157:H7 in pure TSB media. The design of this experiment is similar to studies in which non-immobilized reporter phages are tested for

bacterial sensing; this allows us to compare our finding to the results reported in literature. The electrospun mats were chosen based on their superior performance, as shown in the *E. coli* infection and *E. coli* detection tests (Fig. 4.7, 4.8), in which the phage-immobilized EF mats demonstrated higher infectivity and released higher bioluminescence signals than the other substrates.

In the first step, phage-immobilized EF mats were incubated in a 24-well plate with 1 ml of *E. coli* cultures at cell counts ranging from 10^2 CFU/ml to 10^8 CFU/ml. To quantify detection limit of the sensor, bioluminescence measurements were taken from the resulting lysates every hour (Fig. 4.9).

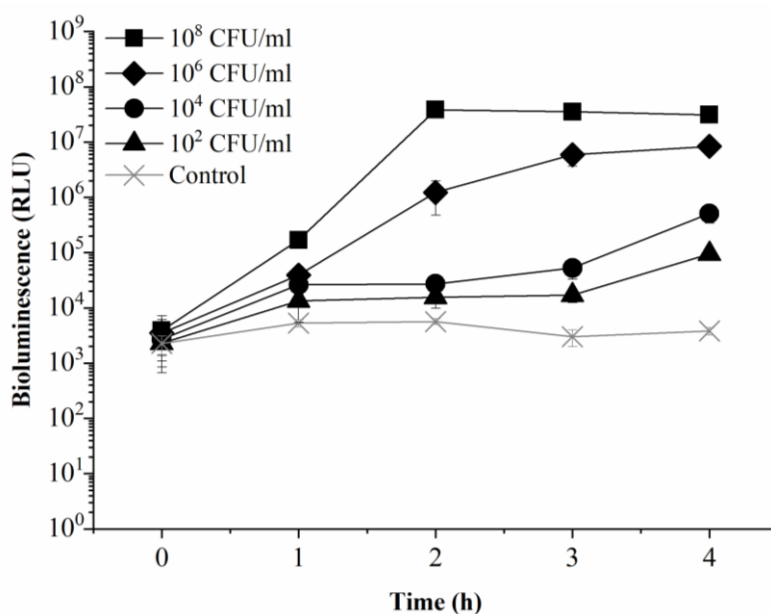


Figure 4.9: Bioluminescence of phage-immobilized EF mats exposed to *E. coli* cultures at various cell counts. No pre-enrichment step was performed prior to incubation. Control is the substrate without *E. coli*. Results were obtained from triplicates and the error reported is based on standard deviations.

The control consisted of the same phage-immobilized substrates immersed in pure TSB media without *E. coli*. It was designed to report the intensity of bioluminescence present from the material itself. The initial bioluminescence was the results of added phage lysate and auto-

bioluminescence of TSB medium. Following the incubation with the phage-immobilized substrates, the bioluminescence intensity of the cultures increased gradually and reached a plateau at different incubation times. Higher signals were observed for wells with higher initial bacterial cell counts. In all cases, infection of *E. coli* O157:H7 cells by reporter phages immobilized on EF mats significantly increased the bioluminescence intensity, even for the lowest host cell counts, even after only 1 h. Thus, the detection limit of the phage-immobilized substrates was found to be equal to or less than 10^2 CFU/ml within 1 hour.

In order to determine if detection could be performed in a different context from the use of flat mats of material, the phage-immobilized PHB substrates were shaped to be used as a swab test based diagnostic tool for the detection of *E. coli* O157:H7. To do so, the experimental method was adapted with slight modifications. First, the range of cell counts was changed to 10^0 CFU/ml to 10^7 CFU/ml to assess the detection range of the phage-based swab test. Next, instead of immersing the phage-immobilized PHB substrates in 10 ml of *E. coli* cultures, the substrates were immersed in 1 ml of *E. coli* dilutions for 1 min (for *E. coli* cell capture), then immediately transferred to 1 ml of sterile TSB medium to initiate the phage infection cycle. The short contact time of phage-to-sample was chosen to utilize rapid detection of the reporter phage-based biosensor.

The first iteration of these experiments was conducted using *E. coli* cultures in pure TSB medium (Fig. 4.10). Next, to measure the ability of the phage-immobilized PHB fibers to detect *E. coli* O157:H7 in a complex food-based medium, the experiments were performed with milk (obtained from local grocery stores) artificially contaminated with controlled amounts of *E. coli* O157:H7 (Fig. 4.11).

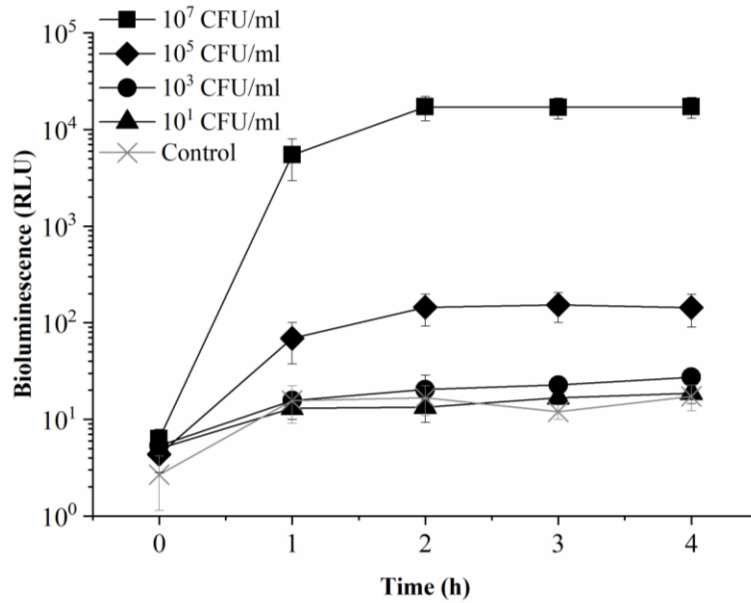


Figure 4.10: Bioluminescence of phage-immobilized electrospun PHB fiber swabs exposed for 1 min to pure TSB medium containing various cell counts of *E. coli* cultures, and incubated in TSB medium at 37°C. Control is the substrate without *E. coli*. Results were obtained from triplicates and the error reported is based on standard deviations.

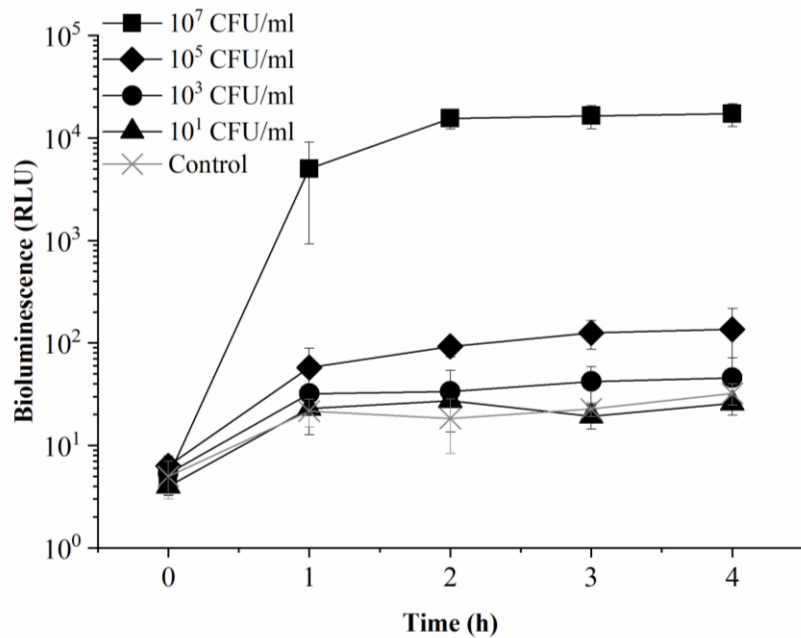


Figure 4.11: Bioluminescence of phage-immobilized electrospun PHB fiber swabs exposed for 1 min to contaminated milk containing various cell counts of *E. coli* cultures, and incubated in TSB medium at 37°C. Control is the substrate without *E. coli*. Results were obtained from triplicates and the error reported is based on standard deviations.

Exponentially growing *E. coli* cells were captured and infected by reporter phages immobilized on EF mats to evaluate the minimum number of cells required to generate a detectable signal thus establish the detection limit. A detectable signal can be produced from an infection between phage-immobilized substrates and 10^5 CFU/ml *E. coli* within 1 h (Fig. 4.10). When available cells per assay (in 1 ml) were below 10^3 , a low level of bioluminescence signal were generated within 3 h.

In contrast to earlier finding (Fig. 4.9), the detection limits of phage-immobilized PHB substrates towards *E. coli* O157:H7 through swab tests (Fig. 4.10, 4.11) were significant higher. The difference can be justified in part by the short contact time (1 min) which may not be enough for detection, as well as limited number of *E. coli* cells transferred to PHB substrates during the 1-min contact time. Bioluminescence signals generated from phage amplification upon infecting the target host cells were governed by multiplicity of infection (MOI). When low amounts of *E. coli* cells were loaded on the PHB substrates, the MOI was greater, resulting in faster wipe-out of the *E. coli* population. It can thus be reasonably assumed that, in such a case, the rate of host lysis outpaces the rate of bacterial replication. Hence, very low amount of Nluc proteins were produced in the phage lysate at the lower cell counts (10 CFU/ml and 10^3 CFU/ml). Further testing would be required to explore the optimal working range and exposure time of the phage-immobilized sensors.

4.10 Phage Attachment on PHB Substrates

In phage immobilization, the density of phages attached to the substrate is one of the major concerns as higher phage loading usually translates into higher bactericide activity, if the phages retain their infectivity after immobilization⁴⁹. Several factors, such as method of immobilization, surface morphology and wettability, can influence the density of phages attached and their activity.

The method of phage immobilization – which could be divided into physical adsorption and chemical immobilization – plays an important role in the properties of the resulting material. Each approach has its own merits and flaws. In the literature, physical adsorption has been shown to result in low surface coverage and heterogeneous surface distribution of the adsorbed phages^{49,60}. This was also observed in the present study through HIM micrographs (Fig. 4.5e, f,h). On the other hand, higher phage packing density has been achieved through covalently binding phages to the substrates^{48,59,108,112}. However, immobilized phages in this manner have been shown to have reduced burst size and longer latent period¹¹³. As a first attempt to immobilize the reporter phage PPO1 on a PHB substrate, physical adsorption was chosen in this work due to its simplicity and its low impact on phage particles. Successful physical adsorption of phages was performed by Bennett et al. in 1997¹¹⁴. In that study, the authors loaded phages on a polystyrene strip to selectively separate *Salmonella* from suspensions of various enterobacteriaceae¹¹⁴. 10 years later, the same method was used by Nanduri to successfully immobilize phages on the gold surface of a quartz crystal microbalance sensor⁴⁰.

The wettability of a substrate also affects phage attachment. Singh et al. showed that phage density was greater on the dextrose- and sucrose-covered gold surfaces than on bare gold surface¹⁰⁸. The researchers claimed that the sugars rendered the surface highly hydrophilic and thus facilitated phage adsorption¹⁰⁸. In another study, plasma treatment was applied on PHB, increasing the hydrophilicity of the polymer⁵⁴. Treated surfaces with immobilized phages were able to wipe out *E.coli* populations faster than untreated surfaces with immobilized phages⁵⁴. Surprisingly, surface roughness was reported to be less important in phage binding. The findings from Tawil et al. showed that modification of surfaces with structurally different thiols had a more profound impact on phage binding than the surface roughness⁴⁸. In contrast to earlier findings, in our work, phage-immobilized electrospun mats retained higher infectivity than solvent-cast films (Fig 4.7), suggesting higher phage loading on the more hydrophobic electrospun mats than the hydrophilic films (Fig 4.2). Presumably, the microstructures of

electrospun mats increase the surface area of phage-loading substrate, allowing more phages attachment to occur, and the void space within the material, enabling phage entrapment. This is in line with observations reported from studies of other electrospun materials, where higher surface area of material led to higher biosensor sensitivity⁷⁸⁻⁸³ and increased loading of particles as compared to flat films¹¹⁵.

The activity of immobilized phages is also of utmost importance in maintaining the functionality of phage-immobilized surfaces. Activity is generally tied to the integrality of the phage particles and the orientation of the immobilized phages⁴⁸. The orientation of immobilized tailed phages can generally be considered tail-up, horizontal, or tail-down⁴⁸. Lysis can only occur when phages are in the tail-up position, as this position renders the phage tail proteins responsible for host recognition available for interaction with host cells, triggering infection⁴⁸. In our work, all phage-immobilized substrates maintained their infectivity towards *E. coli* O157:H7 (Fig. 4.7), suggesting a large portion of the immobilized phages were oriented in the tail-up position. In addition, the infection dynamics of the phage-immobilized electrospun mats had similar trends to those of solvent-cast films reported by Wang et al.⁵⁴, suggesting similar infective profile of immobilized phages, albeit at different rates. However, it is noted that the phages used in both studies were different and may result in different attachment efficiencies due to the amino groups exposed on the capsid surface being different on different phages⁴⁸.

In the present study, results from SEM and HIM (Fig. 4.1, Fig. 4.5), host capture (Fig. 4.8) and infection dynamics (Fig. 4.7) suggest the electrospun fiber mats had the highest phage loading and retain a high level of phage activity compared the three other substrates.

4.11 Comparison of Efficiency of Phage-loaded Substrates

As discussed in the previous section, reporter phage PPO1 were immobilized on the PHB substrates through different mechanisms. Phages bounded to electrospun substrates likely did so through electrostatic bonding and entrapment in mesh networks while electrostatic binding

was the dominant mechanism for phages binding to plasma treated films. Although both mechanisms were based on physical attachment and the phage loading were relatively similar among the substrates, phages immobilized on electrospun PHB were more effective at infecting *E. coli* cells than those immobilized on plasma treated films (Fig. 4.7, 4.8), suggesting higher frequency of phage encounter with host bacteria.

As expected, electrospun membranes outperformed other substrates when considering phage immobilization and infection of host cells. The phage-immobilized EF mats caused population wide lysis within 3 h, faster than any other PHB substrates in the study (Fig. 4.7). Not only that, it also managed to capture more *E. coli* cells, which resulted in the highest bioluminescence signals reported, as compared to other substrates (Fig. 4.8). Therefore, we hypothesize the superior performance of electrospun membranes is due to higher number of phages retained in the mesh network of fibers after the washing cycle (Fig. 4.4). One reason may be the phages were shielded by the hydrophobic PHB fibers thus limiting their contact with the washing liquid.

In these tests, the performance of EB mat followed very closely those obtained with EF mat – both significantly higher than the plasma treated films (Fig. 4.3, 4.7 and 4.8). Although EB mat also display mesh networks similar to those of EF mat, it is hypothesized that the fibers and reduced void fractions produced in EB mat may block the penetration of biological entities, eventually behaving as surface barriers. As compared to EF mat, the EB mat had surfaces densely populated with much smaller fibers and reduced void spaces (Fig. 4.1 a, b). In addition, there were more phages attached around the fibers than the beads, which may also be evidence of lower phage attachment (Fig. 4.5).

The flat films were plasma treated, according to method reported by Wang et al.⁵⁴. Although phages were successfully immobilized through hydroxyl bonding on the surface and exhibit antimicrobial activity, the available phage attachment sites were limited. In addition,

electrostatic repulsion between the charged *E. coli* cells also likely prevented close packing of cells on the surface of films⁵⁷. These combined factors could explain the disparity between the performance of plasma-treated films and electrospun substrates in this study.

4.12 Immobilized Reporter Phages for the Detection of *E. coli* O157:H7

Reporter phages have been used in previous studies to detect *E. coli* in a bioluminescence based assay³⁹. However, only certain types of *E. coli* may pose health risks to the public. Therefore, it is crucial to utilize phages that target specific host strains and leave the benign bacterial population undetected. There is limited literature on phage immobilization or even bioluminescent reporter phages targeting specific *E. coli* strains. Only one study reports the use of a phage-immobilized paper dip assay for the detection of *E. coli* O157:H7, where the bioactive paper strips were used in conjunction with quantitative real-time PCR to determine the presence of the target bacterium in broth and food matrices⁶³. The detection limit of the device was 10 to 50 CFU/ml with a total assay time of 8 h. The list of studies reporting the use of reporter phages towards the detection of *E. coli* O157:H7 is summarized in Table 4.2. To our knowledge, this is the first time where reporter phages were immobilized on polymer substrates for sensing *E. coli* O157:H7.

Table 4.2 Bioluminescent reporter phages for the detection of *E. coli* O157: H7.

Bioreceptor	Detection limit	Time (h)	References
T7	Less than 10 CFU/ml	3	38
phiV10	5-6 cells	7-9	37
Phage lambda, L28	2 CFU/ml	3	34
PP01	1 CFU/ml	6	36

Comparing to these other studies, the detection limit of this phage-immobilized sensor was higher, however, the sensor had a faster response time. Lysogenic bacteriophage phiV10 has been used for the detection of *E. coli* O157:H7 and achieved a detection limit of 5-6 cells³⁷. However, the incubation took 7-9 hours to generate positive signals. In another study, the tailed

lytic phage T7 was used to detect *E. coli* cells in drinking water. The reporter phage detected less than 10 CFU/ml *E. coli* in 3 h of assay time³⁸.

Plasma treated films were previously demonstrated to improve phage binding through electrostatic interactions between the hydroxyl groups and phage capsids⁵⁴. However, the wettability of plasma-treated polymers has been reported to deteriorate overtime. The functional segments on the polymer surface could rearrange to minimize the interfacial energy. As a result, the WCA of modified PHB could increase over time and even revert to its hydrophobic nature. The effect of oxygen plasma on PHB films is thought to last for approximately 1 month¹¹¹. Unlike the time-limited surface treatment, it was shown in this study that electrospun PHB could also function as phage loading substrate through its structure.

Phages immobilized on electrospun mats also displayed a distinctive prolonged phage release compared to the rapid release seen for plasma-treated films. The sustained phage release of the electrospun mats could be advantageous in antimicrobial surface application, where prolonged released of phages is preferred. The small pore sizes of electrospun mats could potentially function as a physical barrier against bacteria entry. Therefore, the phage-immobilized electrospun mats will have a broader scope of application than the flat films. However, despite the advantageous electrospun membranes presented in this work, electrospinning is a more complex process than solvent casting: it requires the material to have certain molecular weight and purity in order to produce smooth fibers.

In this study, the phage-immobilized EF mats were used as swab tests to detect the presence of pathogens. As a biosensor, the device possesses several advantages. First, PHB is biodegradable, making the lifecycle of the sensor environmental friendly. Next, PHB is easily accessible. It can be processed through biomass which makes them a cheaper alternative as compared to metal substrates for biosensor application. The swab test is efficient as it uses small size (0.25 cm²) of the fabricated phage-immobilized PHB substrate and small amounts of

sample (1 ml). Furthermore, the reporter phage Nluc PPO1 targets a specific, pathogenic strain of *E. coli*, leaving the remainder of the microbial population unharmed. The sensor is able to release strong bioluminescence signals upon detecting host cells, leading to a rapid, efficient detection platform.

5. Conclusion

5.1 Summary

Overall, this research focused on designing a reporter phage-based biosensor for the detection of *E. coli* O157:H7 on food products and surfaces. PHB was chosen as the polymer substrate for the support of reporter phage due to its biocompatibility, biodegradability and availability. Phage PPO1, which targets the pathogenic bacterium of interest, was genetically modified to produce the bioluminescent protein Nanoluc and immobilized on PHB substrates. Upon encountering *E. coli* O157:H7, the reporter phage hijacks the bacterial host machinery, producing phage progeny and releasing the Nanoluc protein, which can then be detected through bioluminescence assays.

In this work, PHB was processed through either electrospinning or solvent casting to produce suitable substrates for the biosensor. It was shown that PHB could be processed into a fibrous mats by electrospinning a solution of 5 % w/v polymer in chloroform, whereas a more beaded morphology could be achieved when a 1 % w/v solution was used. In addition, thin films of PHB were fabricated through solvent casting and underwent plasma treatment, according to methods introduced by Wang et al.⁵⁴. The findings from SEM suggested that EF mats were porous. The electrospun mats also had the highest water contact angle measurement in the wettability test, indicative of a more hydrophobic material.

The reporter phages were immobilized on each of the four different substrates produced (two electrospun PHB mats and two solvent-cast PHB films), and the resulting phage-immobilized substrates were characterized. The loading of phages on the materials' surfaces and the release of phages after washing of the surfaces showed that EF mats had the highest phage loading per superficial surface area and reduced phage release after the immobilization, as compared to other substrates. *E. coli* infection dynamics were recorded when phage-immobilized substrates of similar superficial area were immersed in suspensions of *E. coli*

O157:H7. These experiments showed that the phage-immobilized EF mats were more effective at infecting the bacteria, implying higher equivalent multiplicity of infection than the three other substrates. In addition, the *E. coli* capture efficiency of phage-immobilized EF mats was superior to that of other substrates, resulting in strong bioluminescence signals upon exposure to *E. coli* cultures. Based on the results of the SEM, it is possible that EF mats provide a large surface area per volume and a mesh network that enable phage anchoring without affecting phage-bacterium interactions.

Further analysis was done on phage-immobilized EF mats, which showed the most promising result in retaining phage infectivity after immobilization. The samples were studied in detail through fluorescent confocal laser scanning microscopy and helium ion microscopy to understand phage attachment on the fibrous mats. Through the micrographs, phages were seen as clusters located on and around the fibrous structure of PHB, which confirmed the observation done by Naidoo et al⁵⁹.

Next, the bacterial sensing capability of phage-immobilized EF mats was assessed using the bioluminescence assay following exposure to *E. coli* cultures. PHB samples of 0.25 cm² with immobilized reporter phages were immersed in TSB medium and, subsequently, artificially contaminated milk containing various concentrations of *E. coli* for 1 min before being incubated in sterile TSB broth. Bioluminescence measurements were made on samples taken every hour to quantify the detection limit of the sensor. The immobilized phages on electrospun PHB detected *E. coli* cells at a concentration of 10³ CFU/ml within 2 hours in milk, a complex medium.

In summary, this work presents a method to improve phage immobilization on PHB substrates through the production of surface microstructures using electrospinning. Taken together, these findings highlight the use of electrospun PHB as a substrate for reporter phage-based biosensor. The electrospun PHB fiber mats, which are biocompatible, possess high surface area, improve phage immobilization without compromising phage infectivity. This is important

as phage infectivity determines the overall efficiency of many phage applications, be it as antimicrobials or biosensors.

5.2 Significance

The efficiency of any device that harnesses the power of immobilized phages depends on the number and activity of immobilized phages on the device. The basic requirement for designing such devices is to have optimum phage density and activity; hence there is much room for improvements towards making the device better. That being said, the finding from this research, which highlights electrospun polymeric fibrous mats as a better alternative for phage immobilization, makes valuable contributions towards the use of immobilized phages in many applications.

Though the scope of this research is limited to the development of a biosensor incorporating one phage targeting one foodborne pathogen, the importance of this research can be extended due to the abundance of phages that can target different bacterial hosts. For example, immobilized phages can be used for the detection of pathogens and contaminants in food, liquid, environmental and medical settings. Moreover, they have been used to treat localized infections that are hard to cure with normal antibiotics¹¹⁶. In addition, electrospun PHB membranes have been heavily investigated to serve as wound bandage and scaffolding due to its biodegradability and biocompatibility. Products that combine these two technologies may be good candidates for medical purposes.

Other potential applications for immobilized phages include surface disinfection and prevention of biofilm and bacterial growth. Similar to immobilized phages used in wound bandages that provide localized topical treatment, the same technology could work for biofilms as well. Biofilms are collectives of one or more types of microorganisms in which cells stick to each other and surfaces. Bacteria embedded in biofilm are less susceptible to antibiotic treatment and can lead to serious infections. Engineered phages which express an enzyme that

disrupts the biofilm matrix could be attached to electrospun membranes to be used in prevention or treatment¹¹⁷.

5.3 Future Research

The collected results from this research provide a different perspective on phage immobilization on polymer, emphasizing the importance of the substrate's surface morphology. It was shown that electrospun PHB substrates were able to increase efficiency of phage attachment without further modification.

However, in order to realize the full potential of biosensors based on immobilized phages, a few issues should be addressed. First, dehydration, which has damaging effects on immobilized phages, should be addressed. Phages, as bioentities, are robust and can be produced in large amounts with very little investment; however, they can be inactivated upon desiccation¹¹⁸. As water is drawn from phages, osmotic pressure in/out of the phages increase, ultimately destroying them. Micrographs of desiccated phages show detached tails or deformed capsids, which were the main cause of phage losing infectivity¹¹⁸. Leung et al. managed to preserve free phages encapsulated in polysaccharides¹¹⁹. The polysaccharides such as trehalose and pullulan, were reported to stabilize the structures of phages and maintain the shape of the capsid after dessication. If this result could be replicated, it could improve the practicality of phage-based biosensors. In this way, the biosensors could be transferred easily and have a longer shelf life. A preliminary work on long-term stabilization of phages is shown in the Appendices.

Another concern of phage immobilization is the packing density and orientation of phages on the surface. Several studies have underlined the importance of oriented phages to achieve higher packing density without hindering the tail movement. However, the phages used in the studies were often model phages such as T4 or T7, which were not targeting specific strains of pathogenic hosts^{54,120,121}. In this study, micrograph images showed a clustering effect of phages scattered around the PHB fibers, leaving lots of space for increased packing density. Surface

modification such as cationic polymer modification could bind more phages on the fibers, possibly increasing the packing density of phages, leading to an increased efficiency of biosensor.

In conclusion, electrospun PHB were shown to improve phage immobilization, as compared to plasma-treated flat films. The phage-immobilized substrates were shown to function as swab test towards *E. coli* O157:H7 detection. More research is required to realize the full potential of this phage-based device. Interest in phage studies is having a renaissance as they represent a powerful alternative to antibiotics. Given the abundance of phages in the environment, thorough understanding of phages enables us to lend a helping hand from nature in detecting foodborne pathogens such as *E. coli* O157:H7 on food products; ultimately, eliminating disease and sickness and improving the safety of our food production chains.

References

1. Donald, T. 20 Years in Food Safety: A Look Back and Beyond. <https://www.foodqualityandsafety.com/article/20-years-in-food-safety-a-look-back-and-beyond/> (accessed Nov 18, 2019).
2. World Health Organization. "WHO initiative to estimate the global burden of foodborne diseases: fourth formal meeting of the Foodborne Disease Burden Epidemiology Reference Group (FERG): Sharing New Results, Making Future Plans, and Preparing Ground for the Countries." (2014).
3. Uçar, A.; Yilmaz, M. V.; Çakiroglu, F. P. Food Safety – Problems and Solutions. *Significance, Prevention and Control of Food Related Diseases* 2016.
4. Lawan, U.; Iliyasu, Z.; Abubakar, S.; Gajida, A.; Abdussalam, A. Personal and Food Hygiene Practices of Subsistence Food Vendors Operating in Kano Metropolis, Northwestern Nigeria. *International Journal of Medical Science and Public Health* **2015**, 4 (2), 214.
5. Centers for Disease Control and Prevention. Burden of Foodborne Illness: Findings. <https://www.cdc.gov/foodborneburden/2011-foodborne-estimates.html> (accessed Nov 18, 2019).
6. Nebehay, S. Contaminated Food Sickens 1 in 10 People Worldwide Each Year. <https://www.scientificamerican.com/article/contaminated-food-sickens-1-in-10-people-worldwide-each-year/> (accessed Aug 19, 2019).
7. World Health Organization. Food safety. <https://www.who.int/news-room/fact-sheets/detail/food-safety> (accessed Aug 19, 2019).
8. Mitchell, A. Why Food Contamination is a Bigger Problem Than You Realise. <https://thepoultrysite.com/articles/why-food-contamination-is-a-bigger-problem-than-you-realise> (accessed Dec 2, 2019).
9. Library, C. N. N. E. Coli Outbreaks Fast Facts. <https://www.cnn.com/2013/06/28/health/e-coli-outbreaks-fast-facts/index.html> (accessed Aug 19, 2019).
10. Rangel, J. M.; Sparling, P. H.; Crowe, C.; Griffin, P. M.; Swerdlow, D. L. Epidemiology of Escherichia coli O157:H7 outbreaks, United States, 1982-2002. <https://www.ncbi.nlm.nih.gov/pmc/articles/PMC3320345/> (accessed Nov 18, 2019).
11. Scutti, S. Romaine lettuce not safe to eat, CDC says. <https://www.cnn.com/2018/11/20/health/romaine-lettuce-e-coli-cdc/index.html> (accessed Dec 2, 2019)
12. Centers for Disease Control and Prevention. Case Count Maps | Investigation Notice: Multistate Outbreak of E. coli O157:H7 Infections April 2018 | E. coli | CDC. <https://www.cdc.gov/ecoli/2018/o157h7-04-18/map.html> (accessed Aug 19, 2019).
13. Canada, Public Health Agency of Public Health Notice - Outbreak of E. coli infections linked to romaine lettuce. <https://www.canada.ca/en/public-health/services/public-health-notices/2018/outbreak-ecoli-infections-linked-romaine-lettuce.html> (accessed Aug 19, 2019).

14. Bush, L. M.; Perez, M. T.; Last full review/revision April 2018 by Larry M. Bush. Infection by *Escherichia coli* O157:H7 and Other Enterohemorrhagic *E. coli* (EHEC) - Infectious Diseases. <https://www.merckmanuals.com/en-ca/professional/infectious-diseases/gram-negative-bacilli/infection-by-escherichia-coli-0157-h7-and-other-enterohemorrhagic-e-coli-ehec> (accessed Dec 2, 2019).
15. Norwich BioScience Institutes. Why is it so difficult to trace the origins of food poisoning outbreaks? <http://www.sciencedaily.com/releases/2012/06/120601103812.htm> (accessed Nov 18, 2019).
16. Yeo, J. C. C.; Muiruri, J. K.; Thitsartarn, W.; Li, Z.; He, C. Recent Advances in the Development of Biodegradable PHB-Based Toughening Materials: Approaches, Advantages and Applications. *Materials Science and Engineering: C* **2018**, *92*, 1092–1116.
17. World Health Organization. *E. coli*. <https://www.who.int/news-room/fact-sheets/detail/e-coli> (accessed Nov 18, 2019).
18. R M S Research Institute; Ghana Atomic Energy Commission; Accra; Environmental Biology; Health Division; Water Research Institute; Council for Scientific; Industrial Research, (.; Accra; Ghana Stephen T. Odonkor,¹ Joseph K. Ampofo². *1* **2013**, *4*, e2.
19. Lévesque, B.; Gauvin, D. Microbiological Guideline Values for Recreational Bathing in Canada: Time for Change? *Canadian Journal of Infectious Diseases and Medical Microbiology* **2007**, *18* (2), 153–157.
20. Government of Canada, Canadian Food Inspection Agency; Seafood Safety Directorate. Archived - Annex O: Policy on the Control of *E. coli* O157:H7/NM Contamination in Raw Beef Products. <http://www.inspection.gc.ca/food/archived-food-guidance/meat-and-poultry-products/manual-of-procedures/chapter-4/annex-o/eng/1370616273137/1370616333827> (accessed Nov 18, 2019).
21. Schmelcher, M.; Loessner, M. J. Application of Bacteriophages for Detection of Foodborne Pathogens. *Bacteriophage* **2014**, *4* (2).
22. Fratamico, P.; Gehring, A.; Karns, J.; Kessel, J. V. Detecting Pathogens in Cattle and Meat. *Improving the Safety of Fresh Meat* **2005**, 24–55.
23. Chapman, P. Methods available for the detection of *Escherichia coli* O157 in clinical, food and environmental samples. *World Journal of Microbiology and Biotechnology* **2000**, *16*, 733–740.
24. Patient with multidrug-resistant bacterial infection saved by novel phage therapy. <https://health.ucsd.edu/news/releases/Pages/2017-04-25-novel-phage-therapy-saves-patient-with-multidrug-resistant-bacterial-infection.aspx> (accessed Nov 18, 2019).
25. Farooq, U.; Yang, Q.; Ullah, M. W.; Wang, S. Bacterial Biosensing: Recent Advances in Phage-Based Bioassays and Biosensors. *Biosensors and Bioelectronics* **2018**, *118*, 204–216.
26. Nobrega, F. L.; Vlot, M.; Jonge, P. A. D.; Dreesens, L. L.; Beaumont, H. J. E.; Lavigne, R.; Dutilh, B. E.; Brouns, S. J. J. Targeting Mechanisms of Tailed Bacteriophages. *Nature Reviews Microbiology* **2018**, *16* (12), 760–773.

27. Zhou, Y.; Fang, Y.; Ramasamy, R. Non-Covalent Functionalization of Carbon Nanotubes for Electrochemical Biosensor Development. *Sensors* **2019**, *19* (2), 392.
28. Romero-Calle, D.; Benevides, R. G.; Góes-Neto, A.; Billington, C. Bacteriophages as Alternatives to Antibiotics in Clinical Care. *Antibiotics* **2019**, *8* (3), 138.
29. Thouand, G.; Marks, R. *Bioluminescence: Fundamentals and Applications in Biotechnology - Volume 1*; Advances in Biochemical Engineering/Biotechnology; Springer Berlin / Heidelberg: Berlin, Heidelberg, 2014; Vol. 144.
30. Promega Corporation Nano-Glo® Luciferase Assay System Technical Manual. <https://www.promega.com/-/media/files/resources/protocols/technical-manuals/101/nanoglo-luciferase-assay-system-protocol.pdf?la=en> (accessed 25 july, 2019).
31. Close, D.; Xu, T.; Smartt, A.; Rogers, A.; Crossley, R.; Price, S.; Ripp, S.; Sayler, G. The Evolution of the Bacterial Luciferase Gene Cassette (Lux) as a Real-Time Bioreporter. *Sensors* **2012**, *12*(1), 732–752.
32. England, C. G.; Ehlerding, E. B.; Cai, W. NanoLuc: A Small Luciferase Is Brightening Up the Field of Bioluminescence. *Bioconjugate Chemistry* **2016**, *27* (5), 1175–1187.
33. Wood, K. V. The Bioluminescence Advantage. <http://www.promega.ca/resources/pubhub/enotes/the-bioluminescence-advantage/> (accessed 25july, 2019).
34. Ulitzur, N.; Ulitzur, S. New Rapid and Simple Methods for Detection of Bacteria and Determination of Their Antibiotic Susceptibility by Using Phage Mutants. *Applied and Environmental Microbiology* **2006**, *72* (12), 7455–7459.
35. Kim, S.; Kim, M.; Ryu, S. Development of an Engineered Bioluminescent Reporter Phage for the Sensitive Detection of Viable Salmonella Typhimurium. *Analytical Chemistry* **2014**, *86* (12), 5858–5864.
36. Ripp, S.; Jegier, P.; Johnson, C. M.; Brigati, J. R.; Sayler, G. S. Bacteriophage-Amplified Bioluminescent Sensing of Escherichia Coli O157:H7. *Analytical and Bioanalytical Chemistry* **2008**, *391* (2), 507–514.
37. Zhang, D.; Coronel-Aguilera, C. P.; Romero, P. L.; Perry, L.; Minocha, U.; Rosenfield, C.; Gehring, A. G.; Paoli, G. C.; Bhunia, A. K.; Applegate, B. The Use of a Novel NanoLuc -Based Reporter Phage for the Detection of Escherichia Coli O157:H7. *Scientific Reports* **2016**, *6* (1).
38. Hinkley, T. C.; Garing, S.; Singh, S.; Ny, A.-L. M. L.; Nichols, K. P.; Peters, J. E.; Talbert, J. N.; Nugen, S. R. Reporter Bacteriophage T7NLC Utilizes a Novel NanoLuc::CBM Fusion for the Ultrasensitive Detection of Escherichia Coli in Water. *The Analyst* **2018**, *143* (17), 4074–4082.
39. Hazbon, M. H.; Guarin, N.; Ferro, B. E.; Rodriguez, A. L.; Labrada, L. A.; Tovar, R.; Riska, P. F.; Jacobs, W. R. Photographic and Luminometric Detection of Luciferase Reporter Phages for Drug Susceptibility Testing of Clinical Mycobacterium Tuberculosis Isolates. *Journal of Clinical Microbiology* **2003**, *41* (10), 4865–4869.

40. Nanduri, V.; Sorokulova, I. B.; Samoylov, A. M.; Simonian, A. L.; Petrenko, V. A.; Vodyanoy, V. Phage as a Molecular Recognition Element in Biosensors Immobilized by Physical Adsorption. *Biosensors and Bioelectronics* **2007**, *22* (6), 986–992.
41. Gervais, L.; Gel, M.; Allain, B.; Tolba, M.; Brovko, L.; Zourob, M.; Mandeville, R.; Griffiths, M.; Evoy, S. Immobilization of Biotinylated Bacteriophages on Biosensor Surfaces. *Sensors and Actuators B: Chemical* **2007**, *125* (2), 615–621.
42. Horikawa, S.; Bedi, D.; Li, S.; Shen, W.; Huang, S.; Chen, I.-H.; Chai, Y.; Auad, M. L.; Bozack, M. J.; Barbaree, J. M.; Petrenko, V. A.; Chin, B. A. Effects of Surface Functionalization on the Surface Phage Coverage and the Subsequent Performance of Phage-Immobilized Magnetoelastic Biosensors. *Biosensors and Bioelectronics* **2011**, *26* (5), 2361–2367.
43. Yang, L.-M. C.; Diaz, J. E.; Mcintire, T. M.; Weiss, G. A.; Penner, R. M. Covalent Virus Layer for Mass-Based Biosensing. *Analytical Chemistry* **2008**, *80* (4), 933–943.
44. Yang, L.-M. C.; Tam, P. Y.; Murray, B. J.; Mcintire, T. M.; Overstreet, C. M.; Weiss, G. A.; Penner, R. M. Virus Electrodes for Universal Biodetection. *Analytical Chemistry* **2006**, *78* (10), 3265–3270.
45. Handa, H.; Gurczynski, S.; Jackson, M. P.; Auner, G.; Walker, J.; Mao, G. Recognition of Salmonella Typhimurium by Immobilized Phage P22 Monolayers. *Surface Science* **2008**, *602* (7), 1392–1400.
46. Handa, H.; Gurczynski, S.; Jackson, M. P.; Mao, G. Immobilization and Molecular Interactions between Bacteriophage and Lipopolysaccharide Bilayers. *Langmuir* **2010**, *26* (14), 12095–12103.
47. Jia, Y.; Qin, M.; Zhang, H.; Niu, W.; Li, X.; Wang, L.; Li, X.; Bai, Y.; Cao, Y.; Feng, X. Label-Free Biosensor: A Novel Phage-Modified Light Addressable Potentiometric Sensor System for Cancer Cell Monitoring. *Biosensors and Bioelectronics* **2007**, *22* (12), 3261–3266.
48. Tawil, N.; Sacher, E.; Mandeville, R.; Meunier, M. Strategies for the Immobilization of Bacteriophages on Gold Surfaces Monitored by Surface Plasmon Resonance and Surface Morphology. *The Journal of Physical Chemistry C* **2013**, *117* (13), 6686–6691.
49. Shabani, A.; Marquette, C. A.; Mandeville, R.; Lawrence, M. F. Magnetically-Assisted Impedimetric Detection of Bacteria Using Phage-Modified Carbon Microarrays. *Talanta* **2013**, *116*, 1047–1053.
50. Shabani, A.; Zourob, M.; Allain, B.; Marquette, C. A.; Lawrence, M. F.; Mandeville, R. Bacteriophage-Modified Microarrays for the Direct Impedimetric Detection of Bacteria. *Analytical Chemistry* **2008**, *80* (24), 9475–9482.
51. Shabani, A.; Marquette, C. A.; Mandeville, R.; Lawrence, M. F. Carbon Microarrays for the Direct Impedimetric Detection of Bacillus Anthracis Using Gamma Phages as Probes. *The Analyst* **2013**, *138* (5), 1434.

52. Tlili, C.; Sokullu, E.; Safavieh, M.; Tolba, M.; Ahmed, M. U.; Zourob, M. Bacteria Screening, Viability, And Confirmation Assays Using Bacteriophage-Impedimetric/Loop-Mediated Isothermal Amplification Dual-Response Biosensors. *Analytical Chemistry* **2013**, *85* (10), 4893–4901.
53. Hosseinidoust, Z.; Olsson, A. L.; Tufenkji, N. Going Viral: Designing Bioactive Surfaces with Bacteriophage. *Colloids and Surfaces B: Biointerfaces* **2014**, *124*, 2–16.
54. Wang, C.; Sauvageau, D.; Elias, A. Immobilization of Active Bacteriophages on Polyhydroxyalkanoate Surfaces. *ACS Applied Materials & Interfaces* **2016**, *8* (2), 1128–1138.
55. Hao, Y.; Xu, P.; He, C.; Yang, X.; Huang, M.; Xing, J.; Chen, J. Impact of Carbodiimide Crosslinker Used for Magnetic Carbon Nanotube Mediated GFP Plasmid Delivery. *Nanotechnology* **2011**, *22* (28), 285103.
56. Puapermpoonsiri, U.; Spencer, J.; Walle, C. V. D. A Freeze-Dried Formulation of Bacteriophage Encapsulated in Biodegradable Microspheres. *European Journal of Pharmaceutics and Biopharmaceutics* **2009**, *72* (1), 26–33.
57. Hosseinidoust, Z.; Theo G. M. Van De Ven; Tufenkji, N. Bacterial Capture Efficiency and Antimicrobial Activity of Phage-Functionalized Model Surfaces. *Langmuir* **2011**, *27* (9), 5472–5480.
58. Zhou, Y.; Marar, A.; Kner, P.; Ramasamy, R. P. Charge-Directed Immobilization of Bacteriophage on Nanostructured Electrode for Whole-Cell Electrochemical Biosensors. *Analytical Chemistry* **2017**, *89* (11), 5734–5741.
59. Naidoo, R.; Singh, A.; Arya, S. K.; Beadle, B.; Glass, N.; Tanha, J.; Szymanski, C. M.; Evoy, S. Surface-Immobilization of Chromatographically Purified Bacteriophages for the Optimized Capture of Bacteria. *Bacteriophage* **2012**, *2* (1), 15–24.
60. Richter, Ł.; Bielec, K.; Leśniewski, A.; Łoś, M.; Paczesny, J.; Hołyst, R. Dense Layer of Bacteriophages Ordered in Alternating Electric Field and Immobilized by Surface Chemical Modification as Sensing Element for Bacteria Detection. *ACS Applied Materials & Interfaces* **2017**, *9* (23), 19622–19629.
61. Chen, J.; Alcaine, S. D.; Jiang, Z.; Rotello, V. M.; Nugen, S. R. Detection Of Escherichia Coli in Drinking Water Using T7 Bacteriophage-Conjugated Magnetic Probe. *Analytical Chemistry* **2015**, *87* (17), 8977–8984.
62. Jabrane, T.; Dube, M.; Mangin, P. J. Bacteriophage Activity on Paper Surface: Effect of Paper Moisture, 2009, pp 1-6.
63. Anany, H.; Brovko, L.; Dougdoug, N. K. E.; Sohar, J.; Fenn, H.; Alasiri, N.; Jabrane, T.; Mangin, P.; Ali, M. M.; Kannan, B.; Filipe, C. D. M.; Griffiths, M. W. Print to Detect: a Rapid and Ultrasensitive Phage-Based Dipstick Assay for Foodborne Pathogens. *Analytical and Bioanalytical Chemistry* **2017**, *410* (4), 1217–1230.
64. Anany, H.; Brovko, L.; Arabi, T. E.; Griffiths, M. Bacteriophages as Antimicrobials in Food Products. *Handbook of Natural Antimicrobials for Food Safety and Quality* **2015**, 89–116.

65. Anany, H.; Chen, W.; Pelton, R.; Griffiths, M. W. Biocontrol of *Listeria Monocytogenes* and *Escherichia Coli* O157:H7 in Meat by Using Phages Immobilized on Modified Cellulose Membranes. *Applied and Environmental Microbiology* **2011**, *77* (18), 6379–6387.
66. Valle, L. J. D.; Franco, L.; Katsarava, R.; Puiggali, J. Electrospun Biodegradable Polymers Loaded with Bactericide Agents. *AIMS Molecular Science* **2016**, *3* (1), 52–87.
67. Hankermeyer, C. R.; Tjeerdema, R. S. Polyhydroxybutyrate: Plastic Made and Degraded by Microorganisms. In *Reviews of Environmental Contamination and Toxicology*; Ware, G. W., Nigg, H. N. and Doerge, D. R., Eds.; Springer Science+Business Media LCC: New York, **1999**, 1-24.
68. Clark, D. P.; Pazdernik, N. J. *Biotechnology*; Elsevier, AP Cell Press: Amsterdam [u.a.], 2012; , pp 9-20.
69. Mergaert, J.; Wouters, A.; Swings, J.; Anderson, C. In Situ Biodegradation of Poly(3-Hydroxybutyrate) and Poly(3-Hydroxybutyrate-Co-3-Hydroxyvalerate) in Natural Waters. *Canadian Journal of Microbiology* **1995**, *41* (13), 154–159.
70. Finniss, A.; Agarwal, S.; Gupta, R. Retarding Hydrolytic Degradation of Polylactic Acid: Effect of Induced Crystallinity and Graphene Addition. *Journal of Applied Polymer Science* **2016**, *133* (43).
71. Martínez-Tobón, D. I.; Gul, M.; Elias, A. L.; Sauvageau, D. Polyhydroxybutyrate (PHB) Biodegradation Using Bacterial Strains with Demonstrated and Predicted PHB Depolymerase Activity. *Applied Microbiology and Biotechnology* **2018**, *102* (18), 8049–8067.
72. Santos, A. J. D.; Valentina, L. V. O. D.; Schulz, A. A. H.; Duarte, M. A. T. From Obtaining to Degradation of PHB: A Literature Review. Part II. *Ingeniería y Ciencia* **2018**, *14* (27), 207–228.
73. Yeo, J. C. C.; Muiruri, J. K.; Thitsartarn, W.; Li, Z.; He, C. Recent Advances in the Development of Biodegradable PHB-Based Toughening Materials: Approaches, Advantages and Applications. *Materials Science and Engineering: C* **2018**, *92*, 1092–1116.
74. Markl, E. PHB - Bio Based and Biodegradable Replacement for PP: A Review. *Novel Techniques in Nutrition & Food Science* **2018**, *2* (5).
75. Government of Canada, I. Plastics Challenge – Food Packaging. <https://www.ic.gc.ca/eic/site/101.nsf/eng/00036.html> (accessed Aug 16, 2019).
76. Roland-Holst, D.; Triolo, R.; Heft-Neal, S.; Bayrami, B. Bioplastics in California California Department of Resources Recycling and Recovery (*CalRecycle*) 2013.
77. Niaounakis, M. *Biopolymers: Applications and Trends*; William Andrew: Rijswijk, Netherlands;, 2015; , pp 91-138.
78. Su, Z.; Ding, J.; Wei, G. Electrospinning: a Facile Technique for Fabricating Polymeric Nanofibers Doped with Carbon Nanotubes and Metallic Nanoparticles for Sensor Applications. *RSC Adv.* **2014**, *4* (94), 52598–52610.

79. Long, Y.; Chen, H.; Wang, H.; Peng, Z.; Yang, Y.; Zhang, G.; Li, N.; Liu, F.; Pei, J. Highly Sensitive Detection of Nitroaromatic Explosives Using an Electrospun Nanofibrous Sensor Based on a Novel Fluorescent Conjugated Polymer. *Analytica Chimica Acta* **2012**, *744*, 82–91.
80. Long, Y.-Z.; Yu, M.; Sun, B.; Gu, C.-Z.; Fan, Z. ChemInform Abstract: Recent Advances in Large-Scale Assembly of Semiconducting Inorganic Nanowires and Nanofibers for Electronics, Sensors and Photovoltaics. *ChemInform* **2012**, *43* (34).
81. Baranowska-Korczyn, A.; Sobczak, K.; Dłużewski, P.; Reszka, A.; Kowalski, B. J.; Kłopotowski, Ł.; Elbaum, D.; Fronc, K. Facile Synthesis of Core/Shell ZnO/ZnS Nanofibers by Electrospinning and Gas-Phase Sulfidation for Biosensor Applications. *Physical Chemistry Chemical Physics* **2015**, *17* (37), 24029–24037.
82. Cabrita, J.; Ferreira, V.; Monteiro, O. Titanate Nanofibers Sensitized with Nanocrystalline Bi₂S₃ as New Electrocatalytic Materials for Ascorbic Acid Sensor Applications. *Electrochimica Acta* **2014**, *135*, 121–127.
83. Ding, B. Electrospun Nanofibrous Membranes Coated Quartz Crystal Microbalance as Gas Sensor for NH₃ Detection. *Sensors and Actuators B: Chemical* **2004**.
84. Nuraje, N.; Khan, W. S.; Lei, Y.; Ceylan, M.; Asmatulu, R. Superhydrophobic electrospun nanofibers. *Journal of Materials Chemistry A* **2013**, *1*, 1929–1946
85. Bhattarai, R. S.; Bachu, R. D.; Boddu, S. H. S.; Bhaduri, S. Biomedical Applications of Electrospun Nanofibers: Drug and Nanoparticle Delivery. *Pharmaceutics* **2018**, *11*, 5.
86. Garg, K.; Bowlin, G. L. Electrospinning jets and nanofibrous structures. *Biomicrofluidics* **2011**, *5*, 13403.
87. Bera, B. Literature Review on Electrospinning Process (A Fascinating Fiber Fabrication Technique). *Imperial Journal of Interdisciplinary Research (IJIR)* **2016**, *2*, 972–984.
88. Haider, A.; Haider, S.; Kang, I.-K. A Comprehensive Review Summarizing the Effect of Electrospinning Parameters and Potential Applications of Nanofibers in Biomedical and Biotechnology. *Arabian Journal of Chemistry* **2018**, *11* (8), 1165–1188.
89. Megelski, S.; Stephens, J. S.; Chase, D. B.; Rabolt, J. F. Micro- and Nanostructured Surface Morphology on Electrospun Polymer Fibers. *Macromolecules* **2002**, *35*, 8456–8466.
90. Zargham, S.; Bazgir, S.; Tavakoli, A.; Rashidi, A. S.; Damerchely, R. The Effect of Flow Rate on Morphology and Deposition Area of Electrospun Nylon 6 Nanofiber. *Journal of Engineered Fibers and Fabrics* **2012**, *7* (4), 155892501200700.
91. Nurwaha, D.; Han, W.; Wang, X. Investigation of a New Needleless Electrospinning Method for the Production of Nanofibers. *Journal of Engineered Fibers and Fabrics* **2013**, *8*, 155892501300800.
92. Robb, B.; Lennox, B. The Electrospinning Process, Conditions and Control. *Electrospinning for Tissue Regeneration* **2011**, 51–66.
93. Deitzel, J. M.; Kleinmeyer, J.; Harris, D.; Beck Tan, N. C. The effect of processing variables on the morphology of electrospun nanofibers and textiles. *Polymer* **2001**, *42*, 261–272.

94. Sombatmankhong, K.; Suwanton, O.; Waleetorncheepsawat, S.; Supaphol, P. Electrospun fiber mats of poly(3-hydroxybutyrate), poly(3-hydroxybutyrate-co-3-hydroxyvalerate), and their blends. *Journal of Polymer Science Part B: Polymer Physics* **2006**, *44*, 2923-2933
95. Poreskandar, S.; Raeisi, F.; Maghsoodlou, S.; Haghi, A. K. Pathways in Producing Electrospun Nanofibers. In *Pathways to Modern Physical Chemistry*; Wolf, R., Zaikov, G. E. and Haghi, A. K., Eds.; Apple Academic Press: New York, **2016**, 24.
96. Yang, Q.; Li, Z.; Hong, Y.; Zhao, Y.; Qiu, S.; Wang, C.; Wei, Y. Influence of solvents on the formation of ultrathin uniform poly(vinyl pyrrolidone) nanofibers with electrospinning. *Journal of Polymer Science Part B: Polymer Physics* **2004**, *42*, 3721-3726.
97. Pillay, V.; Dott, C.; Choonara, Y. E., et al. A Review of the Effect of Processing Variables on the Fabrication of Electrospun Nanofibers for Drug Delivery Applications. <https://www.hindawi.com/journals/jnm/2013/789289/> (accessed Jul 26, 2019).
98. Baumgarten, P. K. Electrostatic spinning of acrylic microfibers. *Journal of Colloid and Interface Science* **1971**, *36*, 71-79.
99. Chan, S. Y.; Chan, B. Q. Y.; Liu, Z.; Parikh, B. H.; Zhang, K.; Lin, Q.; Su, X.; Kai, D.; Choo, W. S.; Young, D. J.; Loh, X. J. Electrospun Pectin-Polyhydroxybutyrate Nanofibers for Retinal Tissue Engineering. *ACS omega* **2017**, *2*, 8959-8968.
100. Fan, X.; Jiang, Q.; Sun, Z.; Li, G.; Ren, X.; Liang, J.; Huang, T. Preparation and characterization of electrospun antimicrobial fibrous membranes based on polyhydroxybutyrate (PHB). *Fibers and Polymers* **2015**, *16*, 1751-1758.
101. Hosseini, S.; Azari, P.; Jiménez-Moreno, M. F.; Rodriguez-Garcia, A.; Pinguan-Murphy, B.; Madou, M. J.; Martínez-Chapa, S. O. Polymethacrylate Coated Electrospun PHB Fibers as a Functionalized Platform for Bio-Diagnostics: Confirmation Analysis on the Presence of Immobilized IgG Antibodies against Dengue Virus. *Sensors (Basel)* **2017**, *17*.
102. Cold Spring Harbor Protocols. Phosphate-buffered saline (PBS). <http://cshprotocols.cshlp.org/content/2006/1/pdb.rec8247> (accessed Aug 2, 2019)
103. Biswas, N.; Datta, A. 'Coffee-ring' patterns of polymer droplets: chain entanglement effect. *'Coffee-ring' patterns of polymer droplets: chain entanglement effect*, 2014.
104. Ding, Y.; Li, W.; Correia, A.; Yang, Y.; Zheng, K.; Liu, D.; Schubert, D. W.; Boccaccini, A. R.; Santos, H. A.; Roether, J. A. Electrospun Polyhydroxybutyrate/Poly(ϵ -Caprolactone)/Sol-Gel-Derived Silica Hybrid Scaffolds with Drug Releasing Function for Bone Tissue Engineering Applications. *ACS Applied Materials & Interfaces* **2018**, *10* (17), 14540-14548.
105. Correia, D. M.; Ribeiro, C.; Ferreira, J. C. C.; Botelho, G.; Ribelles, J. L. G.; Lanceros-Méndez, S.; Sencadas, V. Influence of electrospinning parameters on poly(hydroxybutyrate) electrospun membranes fiber size and distribution. *Polymer Engineering & Science* **2014**, *54*, 1608-1617.
106. Anbukarasu, P.; Sauvageau, D.; Elias, A. Tuning the Properties of Polyhydroxybutyrate Films Using Acetic Acid via Solvent Casting. *Scientific Reports* **2015**, *5* (1).

107. Morita, M. Characterization of a Virulent Bacteriophage Specific for Escherichia Coli O157:H7 and Analysis of Its Cellular Receptor and Two Tail Fiber Genes. *FEMS Microbiology Letters* **2002**, *211* (1), 77–83.
108. Singh, A.; Glass, N.; Tolba, M.; Brovko, L.; Griffiths, M.; Evoy, S. Immobilization of Bacteriophages on Gold Surfaces for the Specific Capture of Pathogens. *Biosensors and Bioelectronics* **2009**, *24* (12), 3645–3651.
109. Vogler, E. A. Structure and Reactivity of Water at Biomaterial Surfaces. *Advances in Colloid and Interface Science* **1998**, *74* (1-3), 69–117.
110. Sigmund W.M., Hsu SH. (2016) Cassie–Baxter Model. In: Drioli E., Giorno L. (eds) *Encyclopedia of Membranes*. Springer, Berlin, Heidelberg
111. Syromotina, D.; Surmenev, R.; Surmeneva, M.; Boyandin, A.; Nikolaeva, E.; Prymak, O.; Epple, M.; Ulbricht, M.; Oehr, C.; Volova, T. Surface Wettability and Energy Effects on the Biological Performance of Poly-3-Hydroxybutyrate Films Treated with RF Plasma. *Materials Science and Engineering: C* **2016**, *62*, 450–457.
112. Pearson, H. A.; Sahukhal, G. S.; Elasri, M. O.; Urban, M. W. Phage-Bacterium War on Polymeric Surfaces: Can Surface-Anchored Bacteriophages Eliminate Microbial Infections? *Biomacromolecules* **2013**, *14* (5), 1257–1261.
113. Tolba, M.; Minikh, O.; Brovko, L. Y.; Evoy, S.; Griffiths, M. W. Oriented Immobilization of Bacteriophages for Biosensor Applications. *Applied and Environmental Microbiology* **2009**, *76* (2), 528–535.
114. Bennett, A.; Davids, F.; Vlahodimou, S.; Banks, J.; Betts, R. The Use of Bacteriophage-Based Systems for the Separation and Concentration of Salmonella. *Journal of Applied Microbiology* **1997**, *83*(2), 259–265.
115. Sokolova, A. I.; Pavlova, E. R.; Bagrov, D. V.; Klinov, D.; Shaitan, K. Dye Adsorption onto Electrospun Films Made of Polylactic Acid and Gelatin. *Molecular Crystals and Liquid Crystals* **2018**, *669*(1), 126–133.
116. Morozova, V. V.; Vlassov, V. V.; Tikunova, N. V. Applications of Bacteriophages in the Treatment of Localized Infections in Humans. *Frontiers in Microbiology* **2018**, *9*.
117. Harada, L.K.; Silva, E.C.; Campos, W.F.; Del Fiol, F.S.; Vila, M.; Dabrowska, K.; Krylov, V.N.; Balcao, V.M. Biotechnological applications of bacteriophages: State of the art. *Microbiological Research* **2018**, 212-213,38-58.
118. Williams, R.C.; Fraser D. Morphology of the seven T-phages. *Journal of Bacteriology* **1953**, *66*(4), 458-464.
119. Leung, V.; Szewczyk, A.; Chau, J.; Hosseinidoust, Z.; Groves, L.; Hawsawi, H.; Anany, H.; Griffiths, M. W.; Ali, M. M.; Filipe, C. D. M. Long-Term Preservation of Bacteriophage Antimicrobials Using Sugar Glasses. *ACS Biomaterials Science & Engineering* **2017**, *4*(11), 3802–3808.
120. Arya, S. K.; Singh, A.; Naidoo, R.; Wu, P.; McDermott, M. T.; Evoy, S. Chemically immobilized T4-phage for specific Escherichia coli detection using surface plasmon resonance. *Analyst* **2011**, *136*, 486-492.

121. Moghtader, F.; Congur, G.; Zareie, H. M.; Erdem, A.; Piskin, E. Impedimetric detection of pathogenic bacteria with phagephages using gold nanorod deposited graphite electrodes. *RSC Advances*. **2016**, *6*, 97832-97839.
122. Vonasek, E.; Le, P.; Nitin, N. Encapsulation of bacteriophages in whey protein films for extended storage and release. *Food Hydrocolloids* **2014**, *37*, 7-13.

APPENDICES

A. Additional Results

A1. Optimization of Electrospinning

Electrospinning has been used to produce micro- to nano-scaled fiber mats. In order to produce the desired fiber morphology, a few electrospinning parameters were studied and optimised, which included temperature, applied voltage and polymer concentration.

Temperature of the polymer solution was the first studied electrospinning parameter. At room temperature, PHB had low solubility in chloroform and therefore tend to precipitate out from the solvent. This often resulted in clogged nozzle and therefore the electrospinning process had to be arrested. In order to ensure smooth flow of polymer solution, the temperature of polymer solution was kept around 50°C, similar to the value reported by other literatures^{94,100,105}.

Once the polymer solution was kept warm to ensure smooth flow of solution during electrospinning, the applied voltage and polymer concentration were further explored to fine tune the fiber morphology. Polymer solution of 1, 3 and 5 % w/v concentrations were subjected to 5, 10 and 15 kV of applied voltages under the same flow rate of 0.5 ml/h. The electrospun PHB samples produced from the mentioned parameters are shown in Fig. A1.

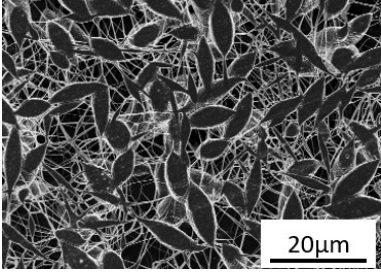
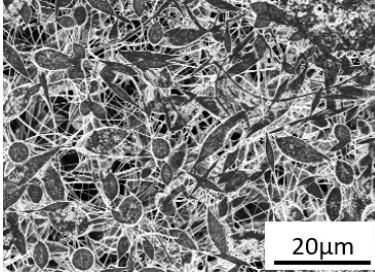
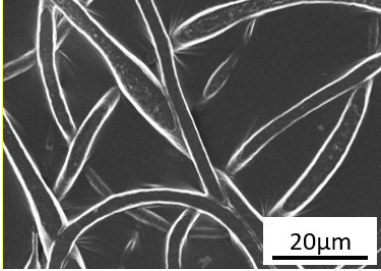
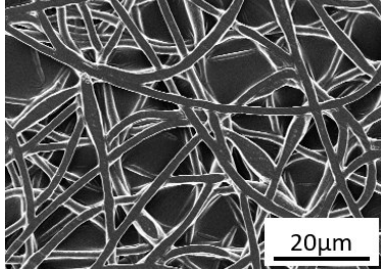
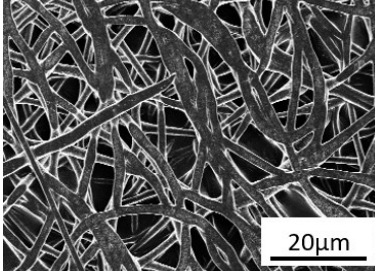
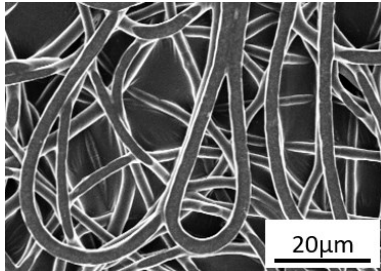
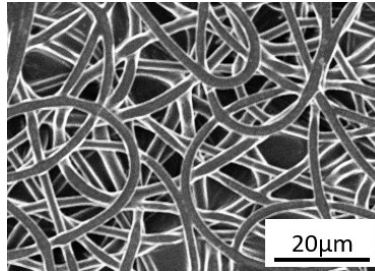
Applied Voltage			
	5 kV	10 kV	15 kV
			
			
			

Figure A1: SEM images of electrospun PHB solution under different conditions.

As shown in Fig. A1, no sample was collected from 1 and 5 % w/v polymer solutions under 5 kV. 1 % w/v polymer solution were fairly insensitive to changes in applied voltage. The solution produced electrospun mats with beaded fibers, regardless of the voltage applied. For 3 % w/v polymer solution, in general, fibers with inconsistent diameter were produced. However, as the applied voltage increased from 5 kV to 15 kV, the spindle like structure gradually disappeared,

resulting in smoother diameter. Fiber structures were obtained from 5 % w/v polymer concentration under 10 and 15 kV. Increasing applied voltage from 10 kV to 15 kV was shown to produce finer fibers with lower diameter.

A2. Dehydration of Phages

Generally, phages were stored at 4 °C as lysate or in deep frozen condition to preserve the virion infectivity. However, to increase the practicality of immobilized-phage based applications, as well as to ease the storage and transportation of phages, infectivity of dehydrated phage PPO1 Nluc was studied in this experiment. Whey protein isolate (WPI) was used to protect the viral particles during the drying process.

Whey protein isolate (as prepared in the reference¹²²) was added to phage lysate and then drop casted and allowed to air-dry overnight at room temperature to form phage films. The phage films were formed by pipetting 100µl of the phage/protectant/deionized water (DI) solution into individual wells of a 24-well plate. The phage titer per film was 5.7×10^9 PFU. The films were stored under ambient conditions for various lengths of time. To quantify the infectivity of encapsulated phages in dried films, the films were dissolved in 1ml of CM buffer (prepared as in reference¹¹⁹) through repeated pipetting. The film solution was serially diluted in CM buffer and used in double agar overlay technique to enumerate phage counts.

The change in infectivity of dried phage PPO1 Nluc was shown in Figure A2.

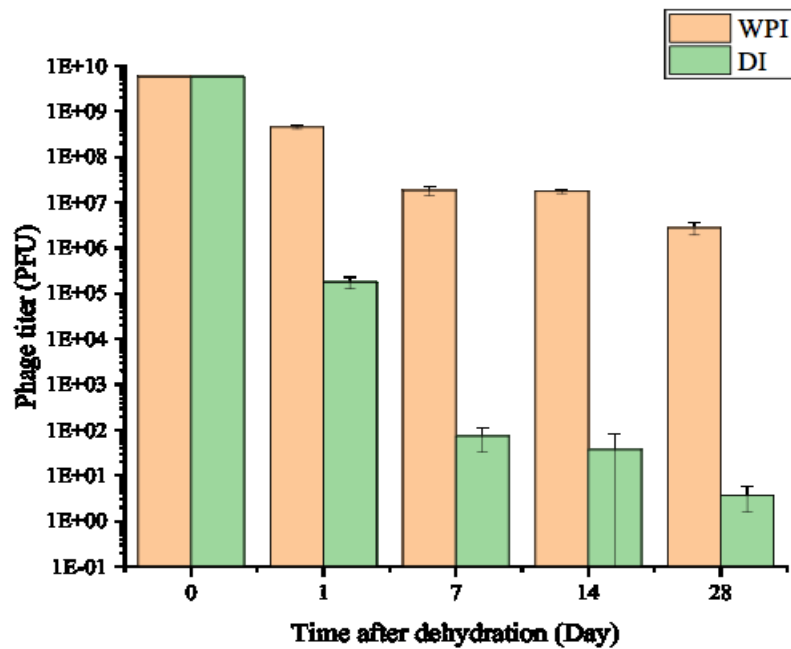


Figure A2: Change of phage titer within 4 weeks of storage at ambient condition. Time (0) is defined as the initial titer of phages in whey protein isolate before drying. Phages encapsulated in whey protein isolate suffered 3 log reduction in phage infectivity after 4 weeks of storage time. Phages encapsulated in deionized water experienced 4 log reduction after 1 day and gradually lost almost all of the activity after 2 weeks.

Appendix B: Permission to Reproduce

- Figure 1.1, which was published by Centers for Disease Control and Prevention, US are not subject to copyright law protections. Permission is not required for use of public domain items.
- Permission to reproduce Figure 2.1, which was published by Franklin L. Nobrega et al. in “Targeting mechanisms of tailed bacteriophages” has been granted by Springer Nature (License # 4702621220722).
- Permission to reproduce Figure 2.2, which was published by Farooq et al. in “Bacterial biosensing: Recent advances in phage-based bioassays and biosensors” has been granted by Elsevier (License # 4702621465241).
- Figure 2.3, which was published by Zhou et al. in “Non-Covalent Functionalization of Carbon Nanotubes for Electrochemical Biosensor Development” has been licensed under a Creative Commons Attribution license (Attribution 2.0 Generic, <https://creativecommons.org/licenses/by/2.0/ca/>)